579370

Sandia National Laboratories
Waste Isolation Pilot Plant

An Update to the WIPP EQ3/6 Database DATA0.FM1 with the Creation of DATA0.FM6

Work Carried Out under the Analysis Plan for WIPP Near-Field Geochemical Process Modeling, AP 200.
To be included in the AP-200 records package

Author: signature on file — Paul S. Domski, Org. 08882 — 5/9/2023 Date

Technical Reviewer: Sungtae Kim — Sungtae Kim, Org. 08881 — 5-9-2023 Date

QA Reviewer: Shelly R. Nielsen — Shelly R. Nielsen, Org. 08880 — 5-9-2023 Date

Management Reviewer: Chammi Miller — Chammi Miller, Org. 08882 — 05/09/23 Date

WIPP:4.4.2.2.1:TD:QA-L:RECERT:579369

Information Only

This page intentionally left blank.

Information Only

TABLE OF CONTENTS

LIST OF TABLES 4
1 INTRODUCTION 5
2 METHODS 8
3 RESULTS 9
4 CONCLUSIONS 29
5 REFERENCES 30
APPENDIX A. Updates and Additions to DATA0.FM1 to Create DATA0.FM6 35

Information Only

LIST OF TABLES

Table 1. Abbreviations, Acronyms, and Initialisms. 5

Table 2. Solubility Products and Aqueous Dissociation Constants for Reactions with Lead that will be included in DATA0.FM6....9

Table 3. Pitzer Interaction Parameters for the Lead system that will be included in DATA0.FM6....10

Table 4. Apparent Log K Values for Anglesite. 13

Table 5. Apparent Log K Values for Abellaite. 15

Table 6. Equilibrium Constants for Reactions with Iron that will be included in DATA0.FM6....16

Table 7. Pitzer Interaction Coefficients (Cation-Anion Interactions) for Ions Containing Iron that will be included in DATA0.FM6 17

Table 8. Pitzer Interaction Coefficients (Cation-Cation Interactions) for Ions Containing Iron that will be included in DATA0.FM6 17

Table 9. Pitzer Interaction Coefficients (Cation-Cation-Anion Interactions) for Ions Containing Iron that will be included in DATA0.FM6 17

Table 10. Apparent Log Ksp values for Hibbingite....19

Table 11. Apparent Log Ksp values for Ferrous Hydroxide. 19

Table 12. Apparent Log Ksp values for Chukanovite. 20

Table 13. Reactions and log K values at 25 °C and I = 0 used for the Mg-Oxalate system. 22

Table 14. Apparent Log K values for Glushinskite. 23

Table 15. Solubility constant of Earlandite ($Ca_3(Citrate)_2 \cdot 4H_2O$) to be implemented in DATA0.FM6....24

Table 16. Recommendation of new Pitzer parameters for the $Nd(OH)_3(s)$ - $MgCl_2$ - H_2O system. 25

Table 17. Apparent Log K values for $Am(OH)_3(am)$. 26

Table 18. Comparison of the documented parameters with those estimated using DATA0.FM6....28

Information Only

1 INTRODUCTION

The objective of this analysis report is to document the addition of parameters to a current quality-assured WIPP EQ3/6 thermodynamic database, DATA0.FM1 (Xiong, 2011), to create new quality-assured EQ3/6 thermodynamic database, DATA0.FM6. This new database is intended to be used for calculating actinide solubility values for the Replacement Panels Planned Change Request (RPPCR) and the 2024 Compliance Recertification Application (CRA-2024). The motivation behind creation of this database is to enhance chemical systems currently included in DATA0.FM1, to include new chemical systems that may impact actinide solubility, and to account for the effects of elements that have large inventories in the WIPP repository, such as iron and lead. In doing so the U.S. Department of Energy (DOE) will have addressed Issues 5, 8, 29, and 32 of the U.S. Environmental Protection Agency (EPA) (Peake, 2022). This analysis report, as per NP 9-1, Revision 10, is considered a compliance decision analysis.

The new QA database, DATA0.FM6, will include model parameters derived under AP-190 (Jang et al., 2021a). In addition, literature searches were performed to determine the availability of published data/parameters that are suitable for WIPP conditions, these data/parameters are listed in Miller et al. (2023) and the following sections. By using the currently verified QA EQ3/6 thermodynamic database, DATA0.FMT.R2, also known as DATA0.FM1 (Xiong, 2011) as the starting database additional parameters were added and tested. The EPA Issue 5 (Peake, 2022) regarding the EDTA model included in DATA0.FM4 (Domski, 2019) and DATA0.FM5 (Domski, 2020) has been resolved by use of the DATA0.FM1 EDTA model which the EPA agreed to at the October 25, 2022 Technical Exchange.

The purpose of this analysis report is not to document or discuss the chemical systems of the starting database, DATA0.FM1, nor is it to critically evaluate the parameters being added to create DATA0.FM6. For further information the reader is directed to GEOC 21-11 (Jang et al., 2021b) and GEOC 22-01 (Jang and Foli, 2023).

Table 1 defines the abbreviations, acronyms, and initialisms used in this report. Abbreviations, Acronyms, and Initialisms.

Table 1. Abbreviations, Acronyms, and Initialisms.

Abbreviation, Acronym, or Initialism	Definition
Ac, acetate	CH_3COO^- or $CH_3CO_2^-$
Am, Am(III)	americium, americium in the +III oxidation state
am	amorphous
anhydrite	$CaSO_4$
AP	analysis plan

Information Only

Aq	aqueous
aragonite	$CaCO_3$,a polymorph of $CaCO_3$ that is metastable with respect to calcite
Atm	atmosphere(s)
B, B(III)	boron, boron in the +III oxidation state
Br, Br(−I)	bromine, bromine in the −I oxidation state
Brucite	$Mg(OH)_2$
C	carbon
Ca, Ca(II), Ca^{2+}	calcium, calcium in the +II oxidation state, calcium ion
CAR	Per NP 16-1, Revision 7, Corrective Action Request
Calcite	$CaCO_3$, the thermodynamically stable polymorph of $CaCO_3$
Cerussite	$PbCO_3$
Cit, citrate	$(CH_2COO)_2C(OH)(COO)^{3-}$ or $(CH_2CO_2)_2C(OH)(CO_2)^{3-}$
Cl, Cl(−I), Cl^-	chlorine, chlorine in the −I oxidation state, chloride ion
CMS	(Sandia/WIPP software) Configuration Management System
CO_2	carbon dioxide
CO_3^{2-}	carbonate
cr	crystalline
CRA-2004	the first WIPP Compliance Recertification Application, submitted to the EPA in March 2004
CRA-2009	the second WIPP Compliance Recertification Application, submitted to the EPA in March 2009
CRA-2014	the third WIPP Compliance Recertification Application, to be submitted to the EPA in March 2014
DB	(thermodynamic) database
DBR	direct brine release
dolomite	$CaMg(CO_3)_2$, a carbonate mineral that nucleates and grows slowly under low-temperature conditions and is often suppressed (prevented from forming) in geochemical modeling calculations
DRZ	disturbed rock zone
EDTA	ethylenediaminetetraacetate, $(CH_2COO)_2N(CH_2)_2N(CH_2COO)_2)^{4-}$ or $(CH_2CO_2)_2N(CH_2)_2N(CH_2CO_2)^{4-}$
EPA	(U.S.) Environmental Protection Agency
EQ3/6	a geochemical software package for speciation and solubility calculations (EQ3NR) and reaction-path calculations (EQ6)
earlandite	$Ca_3[C_3H_5O(COO)_3]_2 \cdot 4H_2O$
ERDA-6	Energy Research and Development Administration (WIPP Well) 6, a synthetic brine representative of fluids in Castile brine reservoirs
f_{CO_2}	fugacity (similar to the partial pressure) of CO_2
Fm.	Formation
GWB	Generic Weep Brine, a synthetic brine representative of intergranular Salado brines at or near the stratigraphic horizon of the repository
Gypsum	$CaSO_4 \cdot 2H_2O$
H or H_2, H^+	hydrogen or hydrogen ion
Halite	NaCl
H_2O	water (aq, g, or contained in solid phases)
hydromagnesite	$Mg_5(CO_3)_4(OH)_2 \cdot 4H_2O$

Information Only

I	ionic strength, defined by $I = ½ \times \Sigma_i(M_i \times z_i^2)$, in which M_i and z_i are the molarity and charge of species i
I/O	input/output
K, K(I)	potassium, potassium in the +I oxidation state
Kg	kilogram(s)
Lead oxalate	$PbC_2O_4(cr)$
litharge	PbO
M	Molar, $mol \cdot dm^{-3}$
m	meters or molal, $mol \cdot kg^{-1}$
magnesite	$MgCO_3$
Mg, Mg(II)	magnesium, magnesium in the +II oxidation state
MgO	magnesium oxide, used to refer to the WIPP engineered barrier, which includes periclase as the primary constituent and various impurities
mM	millimolar
Na, Na(I), Na^+	sodium, sodium in the +I oxidation state, sodium ion
nesquehonite	$MgCO_3 \cdot 3H_2O$
Np, Np(V)	neptunium, neptunium in the +V oxidation state
O or O_2	oxygen
OH, OH^-	hydroxide or hydroxide ion
Ox, oxalate	$(COO)_2^{2-}$ or $C_2O_4^{2-}$
PA	performance assessment
PABC	Performance Assessment Baseline Calculations
Pb, Pb(II)	Lead, lead in the +II oxidation state
periclase	pure, crystalline MgO, the primary constituent of the WIPP engineered barrier
pH	the negative, common logarithm of the activity of H^+
Phase 3	$Mg_2Cl(OH)_3.4H_2O$
Phase 5	$Mg_3Cl(OH)_5.4H_2O$
pcH	the negative, common logarithm of the molar concentration of H^+
polyhalite	$K_2MgCa_2(SO_4)_4 \cdot 2H_2O$
QA	quality assurance
Rev.	revision
RH	relative humidity
S, S(VI), SO_4^{2-}	sulfur, sulfur in the +VI oxidation state, sulfate ion
SCA	S. Cohen and Associates
SNL	Sandia National Laboratories
Th, Th(IV)	thorium, thorium in the +IV oxidation state
TIC	total inorganic C
U, U(IV), U(VI)	uranium, uranium in the +IV oxidation state, uranium in the +VI oxidation state
whewellite	$CaC_2O_4 \bullet H_2O$
WIPP	Waste Isolation Pilot Plant
wt %	weight percent

Information Only

2 METHODS

This analysis report documents the steps used to create a quality assured model parameter database, DATA0.FM6, in accordance with AP-200 (Domski, 2022). For the parameters documented in GEOC 21-11 (Jang et al., 2021b), GEOC 22-01 (Jang and Foli, 2023), memoranda associated with GEOC-22-01 (Jang, 2022, 2023a,b), and summarized in Miller et al. (2023) the following steps were followed in updating the database:

1) Copy and rename DATA0.FM1 (Xiong 2011) to DATA0.FM6.
2) Edit DATA0.FM6 and enter the parameters, and parameter updates as listed in Miller et al. (2023).
3) Parameter verification will be demonstrated by graphically comparing the EQ3/6 simulated model response to the measured data used to fit those parameters, also called "training" data. Both comparisons of the simulated model response to the solubility measurements and the apparent log Ksp [1]values are included. For the cases presented herein, the apparent log Ksp values based on experimental data required no modeling results or assumptions other than the stoichiometry of the solid phase. For parameters that were estimated using the Python parameter fitting script (Kirchner, 2012) the scripts were re-run using DATA0.FM6 and the fitted parameter values were compared to the values in the respective source documents to insure the new database can reproduce the original values within the acceptance criteria outlined in Section 3. This is not a validation exercise, but rather a verification exercise to demonstrate that the parameters and codes used herein, and in the respective source memos, yield results consistent with the measured data used in the parameter derivations.

Comparisons of the model response using DATA0.FM6 to independent experimental data not used for parameter fitting, so called "test" data is beyond the scope of this analysis, and is not be presented. Herein the model is compared to the training data, which is termed training-data-model comparison.

[1] The EPA, during the CRA-2019 DPA completeness evaluation, requested the DOE provide a comparison of the apparent Log K values calculated from the measured and the simulated data as a metric to evaluate the Log K values of solids and aqueous species in the WIPP database, therefore, this method was carried forth in the current report.

Information Only

3 RESULTS

3.1 GEOC 21-11 and GEOC 22-01 Parameters

The following sections summarize the changes and additions that are included in DATA0.FM6. The model parameters that were added in the creation of DATA0.FM6 are documented in GEOC 21-11 (Jang et al., 2021b) and GEOC 22-01 (Jang and Foli, 2022), and these parameters are also summarized in Miller et al. (2023). Files used or created for this exercise include EQ3NR input and output files, an Excel spreadsheet, and the thermodynamic database DATA0.FM6. These files are stored at: /data/cvs/CVSLIB/WIPP_EXTERNAL/ap200/Files.

3.1.1 The Lead System

The lead system as presented in Jang (2021, 2022, and 2023), Jang et al. (2021b, and Jang and Foli (2023) is included in DATA0.FM6. Inclusion of a Pitzer based lead-chloride model in the WIPP database addresses the EPA Issue 8 (Peake, 2022), additional Pitzer based lead systems may be added in the future.

This section, Tables 2 and 3, provide the parameters for the lead systems that will be included in DATA0.FM6.

Table 2. Solubility Products and Aqueous Dissociation Constants for Reactions with Lead that will be included in DATA0.FM6

Reaction	log K	Source
Solid Dissolution Reactions		
$PbCl_2(s)$ (Cotunnite) $\rightleftharpoons Pb^{2+} + 2Cl^-$	-4.83	Edwards et al. (1992) and Jang (2021)
$PbCO_3(s)$ (Cerussite) + $H^+ \rightleftharpoons Pb^{2+} + HCO3^-$	-2.85	Powell et al. (2009)
$NaPb_2(CO_3)_2(OH)(s)$ (Abellaite) + $3H^+ \rightleftharpoons Na^+ + 2Pb^{2+} + 2HCO_3^- + H_2O$	2.59	Jang (2022)
$2Pb(CO_3)_2.Pb(OH)_2(s)$ (Hydrocerussite) + $4H^+ \rightleftharpoons 3Pb^{2+} + 2HCO_3^- + 2H_2O$	2.41	Edwards et al. (1992)
$PbSO_4(s)$ (Anglesite) $\rightleftharpoons Pb^{2+} + SO_4^{2-}$	-7.77	Jang (2023)
Aqueous Dissociation Reactions		
$PbCl^+ \rightleftharpoons Pb^{2+} + Cl^-$	-1.48	Millero and Byrne (1984)
$PbCl_2(aq) \rightleftharpoons Pb^{2+} + 2Cl^-$	-2.03	Millero and Byrne (1984)
$PbCl_3^- \rightleftharpoons Pb^{2+} + 3Cl^-$	-1.86	Millero and Byrne (1984)
$PbHCO_3^+ \rightleftharpoons Pb^{2+} + HCO_3^-$	-1.86	Powell et al. (2009)
$PbCO_3(aq) + H^+ \rightleftharpoons Pb^{2+} + HCO_3^-$	3.88	Powell et al. (2009)
$Pb(CO_3)_2^{2-} + 2H^+ \rightleftharpoons Pb^{2+} + 2HCO_3^-$	10.53	Powell et al. (2009)
$Pb(CO_3)OH^- + 2H^+ \rightleftharpoons Pb^{2+} + HCO_3^- + H_2O$	13.42	Powell et al. (2009)

Information Only

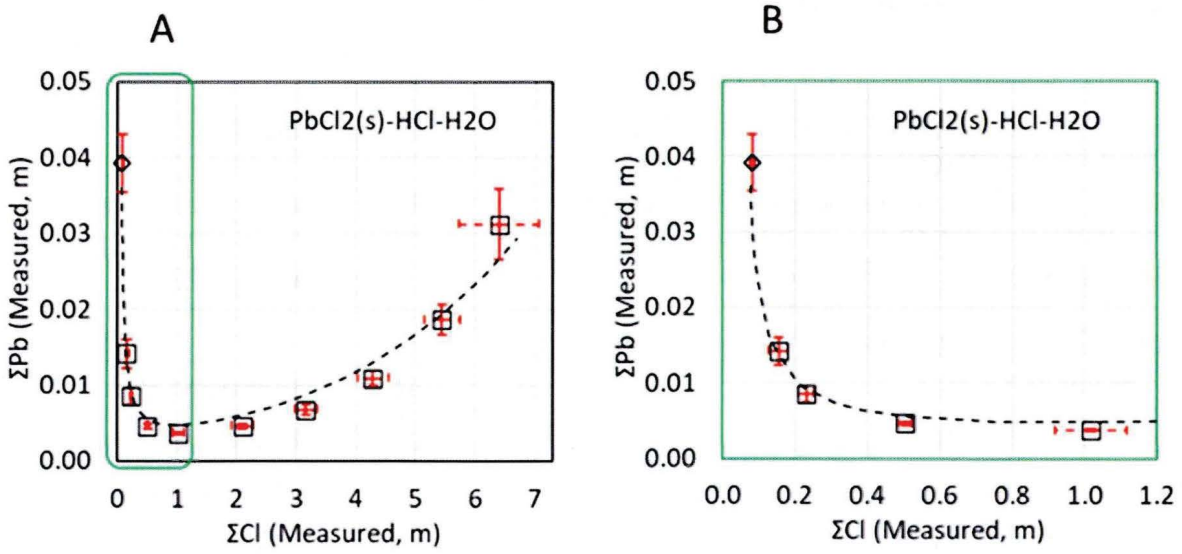
Reaction	log K	Source
$Pb(CO_3)_3^{4-} + 3H^+ \rightleftharpoons Pb^{2+} + 3HCO_3^-$	27.19	Jang (2022)

Table 3. Pitzer Interaction Parameters for the Lead system that will be included in DATA0.FM6

I	*j*	α_1/α_2	$\beta^{(0)}$	$\beta^{(1)}$	$\beta^{(2)}$	C^{φ}	Source
H^+	$PbCl_3^-$	2.0/12.0	0.1077	0.0425	0.00	-0.0035	Jang (2021)
Na^+	$PbCl_3^-$	2.0/12.0	-0.10025	0.0	0.0	0.0	Jang et al. (2021b)
Mg^{2+}	$PbCl_3^-$	2.0/12.0	0.230125	0.0	0.0	0.0	Domski (2023) after Jang et al. (2021b)[2]
i	***j***	θ_{ij}					**Source**
H^+	Pb^{2+}	0.343					Jang (2023a)

The Lead – Chloride – Sodium – Magnesium Model

Jang et al. (2021b) and Jang and Foli (2023) adapted the solubility of $PbCl_2$(s) (cotunnite) from Edwards et al. (1992), and Millero and Byrne (1984) model for the Pb^{2+} – Cl^- aqueous complexes as the basis of this chemical system. The model was adapted to the Pitzer model by fitting and inclusion of the binary Pitzer parameters for the pairs H^+ / $PbCl_3^-$, Na^+ / $PbCl_3^-$ and Mg^{2+} / $PbCl_3^-$, and the cation – cation Pitzer parameter θ for the H^+ / Pb^{2+} pair. Figures 1 – 3 display the visual comparison of the H^+ - Pb^{2+}, Na^+ - Pb^{2+}, and Mg^{2+} - Pb^{2+} systems, respectively.



[2] The value of θ for Mg^{2+} - $PbCl^{3-}$ in Jang et al. (2021b) contains a transcription error, the correct value is documented in Domski (2023), and Table 3 above.

Information Only

Figure 1. Reproduction of Figure V.2-7, Jang et al. (2021b) displaying the model prediction compared to the training data for the $PbCl_2(s) – HCl – H_2O$ system. Figure A shows the entire concentration range investigated. Figure B shows a zoomed-in view of the area marked with the green rectangle in Figure A. The binary Pitzer parameter $\beta^{(0)}$ for the H^+ / $PbCl_3^-$ pair was the fitting parameter adjusted using the data in this figure.

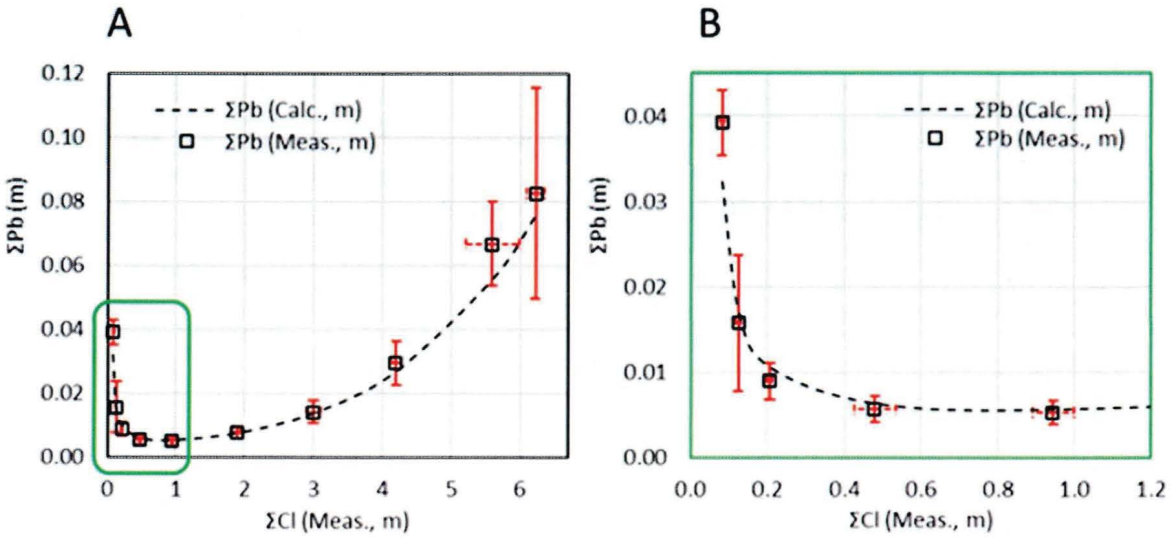


Figure 2. Reproduction of Figure V.3-9 C & D from Jang et al. (2021b) showing parametrization of the $PbCl_2(s) – NaCl – H_2O$ system. Figure A shows the entire concentration range investigated. Figure B shows a zoomed-in view of the area marked with the green rectangle in Figure A. The binary Pitzer parameter $\beta^{(0)}$ for the Na^+ / $PbCl_3^-$ pair was the fitting parameter.

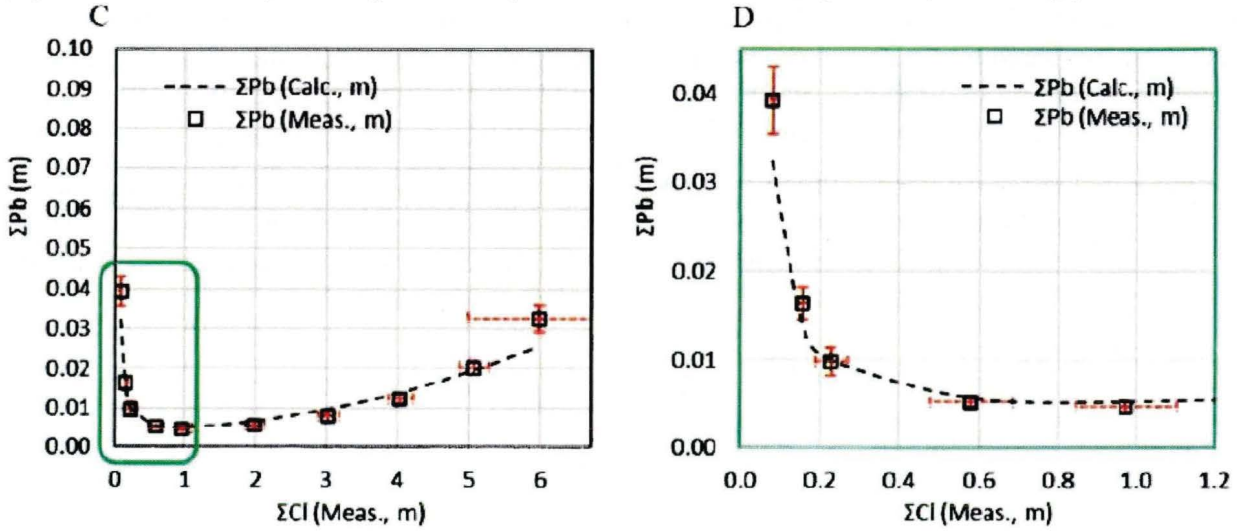


Figure 3. Reproduction of Figure V.4-9 C & D from Jang et al. (2021b) showing parametrization of the $PbCl_2(s) – MgCl_2 – H_2O$ system. Figure C shows the entire concentration range investigated. Figure D shows a zoomed-in view of the area marked with the green rectangle in Figure A. The binary Pitzer parameter $\beta^{(0)}$ for the Mg^{2+} / $PbCl_3^-$ pair was the fitting parameter.

Information Only

Jang et al. (2021b) demonstrated that the lead – sodium – magnesium - chloride aqueous speciation model of Millero and Byrne (1984) and the lead – chloride solid phase (cotunnite) model of Edwards et al. (1992) could be used at ionic strengths up to 6 molal with the addition of the binary Pitzer pairs for H^+ / $PbCl_3^-$, Na^+ / $PbCl_3^-$ and Mg^{2+} / $PbCl_3^-$. Figures 1 through 3 show that Jang et al.'s (2021b) lead – chloride models fit the training data well.

The Lead – Sulfate System

Jang (2023a) parametrized the solubility measurements of Anglesite ($PbSO_4(s)$) in solutions of increasing concentrations of Na_2SO_4 from 0.01 to 1.8 m at constant 0.15 m NaCl. The log K value of anglesite from Powell et al. (2009) was used in the analysis, and the cation – cation Pitzer parameter, θ, for the H^+ / Pb^{2+} pair was fit to match the experimental data. The experimental data and the resulting fit are shown in Figure 4.

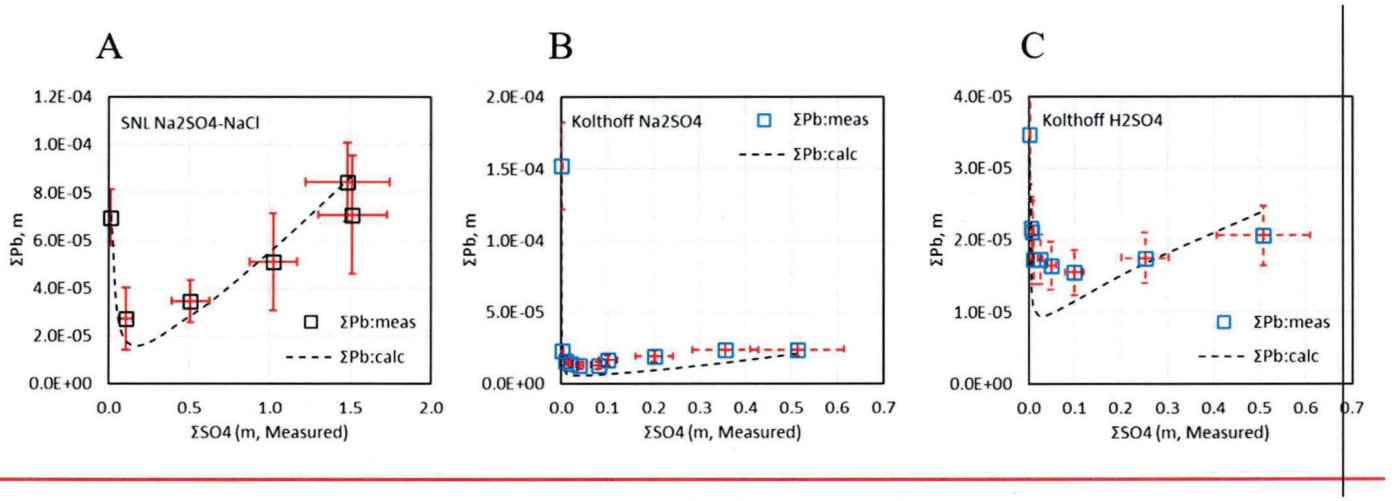


Figure 4. Reproduction of Figure VIII-5 from Jang (2023a). Figure A shows the model prediction compared to the SNL measured data for the $PbSO_4$ system.. Figures B and C show the measured data of Kolthoff et al. (1942) in Na_2SO_4 and H_2SO_4 solutions, respectively, together with the model fit. Fitting parameter is the cation-cation Pitzer parameter θ for the H^+ / Pb^{2+} pair.

The log K value for Anglesite ($PbSO_4(s)$) calculated by Jang (2023a) used the measured data of Kolthoff et al. (1942), and used this data and EQ3NR to calculate the Pitzer activity coefficients for Pb^{2+} and SO_4^{2-}. Jang (2023a) then calculated the Pitzer-based equilibrium constant for the dissolution of Anglesite via,

$$PbSO_4(s) \rightleftharpoons Pb^{2+} + SO_4^{2-}$$

$$K = \gamma_{Pb2+}[Pb^{2+}] + \gamma_{SO42-}[SO_4^{2-}]$$

Where γ_i = the activity coefficient of species i, and $[i]$ is the molality of species i

Jang (2023a) improved the fit of the log K value to the measured data by fitting the Pitzer cation-cation θ parameter for the H^+ / Pb^{2+} pair. See Jang (2023a) for a detailed discussion of this choice of parameters. The verification of the Pitzer parameter and log K values for the lead – sulfate system are plotted in Figure 4 A, B, and C above.

Information Only

To gain further confidence in the anglesite solubility product its apparent solubility product from the experimental data (Table VIII-2, Jang, 2023a) and that calculated from the EQ3NR model response were graphically compared. The results are plotted in Figure 5, and the method used to calculate the apparent log K is presented below.

The dissolution reaction for anglesite can be written as:

$$PbSO_4(s) \rightleftharpoons Pb^{2+} + SO_4^{2-}$$

The apparent solubility product, Ksp,app, for the dissolution of anglesite follows:

$$Ksp,app = [Pb^{2+}] \times [SO_4^{2-}]$$

By definition, the activity of a pure solid is equal to 1. The activity of water is set here to be equal to 1 for simplicity of calculation of Ksp,app. Note the square brackets ([-]) indicate concentration in units of molality (m). The log of the apparent solubility product is then given by:

$$\log Ksp,app = \log[Pb^{2+}] + \log[SO_4^{2-}]$$

Table 4 provides the pmH, Pb, and sulfate molality values used to calculate the log Ksp,app values for anglesite for the experimental and simulated values.

Table 4. Apparent Log K Values for Anglesite.

Measured Data from Jang (2023a), Table VIII-2				**EQ3NR Simulated Data**			
pmH	**Pb(m)**	**SO_4(m)**	**log Ksp,app**	**pmH**	**Pb(m)**	**SO_4(m)**	**log Ksp,app**
2.74	6.95E-05	1.22E-02	-6.07	2.74	1.22E-02	1.64E-01	-6.07
3.06	2.74E-05	1.06E-01	-5.54	3.06	1.06E-01	3.35E-01	-5.72
3.21	3.46E-05	5.07E-01	-4.76	3.21	5.07E-01	1.08E+00	-4.84
3.17	5.10E-05	1.02E+00	-4.28	3.17	1.02E+00	2.15E+00	-4.24
3.26	7.06E-05	1.51E+00	-3.97	3.33	1.48E+00	3.07E+00	-3.89
3.33	8.44E-05	1.48E+00	-3.90	3.26	1.51E+00	3.04E+00	-3.89

Information Only

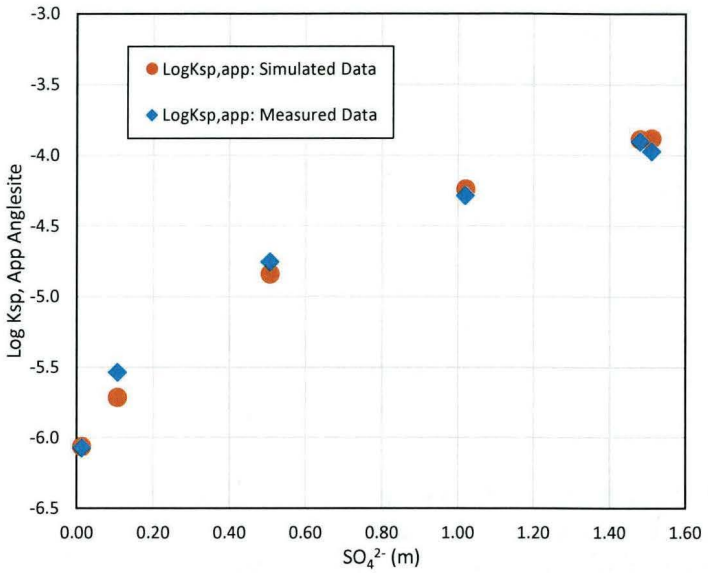


Figure 5. Apparent Log Ksp values for the anglesite measured data compared to the model predicted apparent Log Ksp values.

The Lead – Carbonate System

Jang (2022) revisited the lead -carbonate experimental data of Kirkes et al. (2014 a, b, and c) and the parameterization of this data by Xiong (2015a, b). The result was the identification of the sodium – lead carbonate phase, $NaPb_2(CO_3)_2(OH)(s)$ (abellaite), and the fitting of its solubility product. See Jang (2022) for details. Jang (2022) provided verification of the Abellaite solubility model in Figure VIII-6 therein, which is reproduced below as Figure 6.

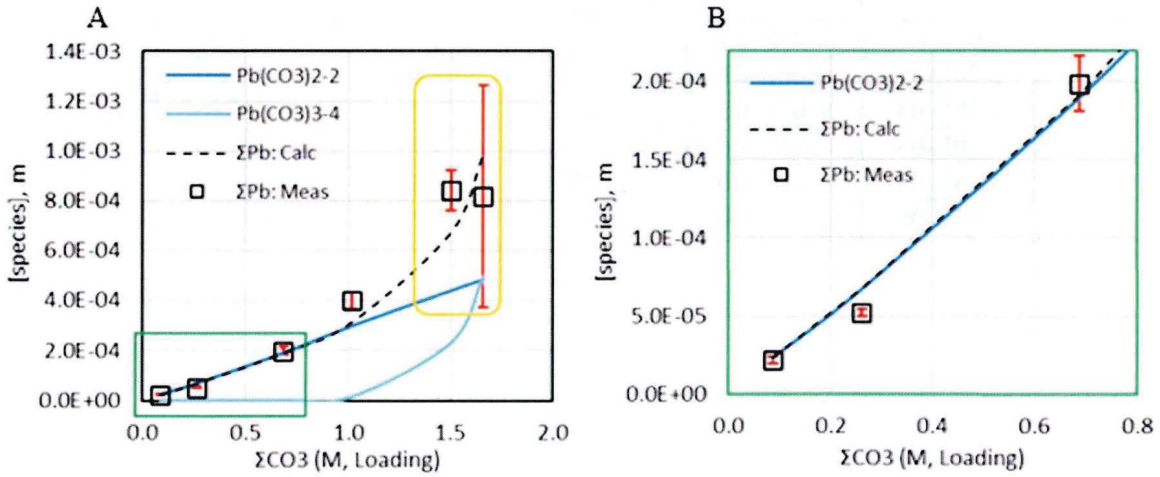


Figure 6. Reproduction of Figure VIII-6 of Jang (2022). Model prediction with log K(abellaite) = 2.59, and log $K(Pb(CO_3)_3^{4-})$ = 27.19. See Jang (2022) for details and an explanation of the yellow rectangle in A.

For CRA-2019 DPA Domski and Sisk-Scott (2019) reported that for the GWB and ERDA-6 brines the total inorganic carbon (TIC) concentration decreased from 0.016 M to 2.5E-04 M for unreacted and reacted brines, respectively. In other words, lower than the TIC range specified by Jang (2022).

Information Only

To build confidence in the abellaite solubility product its apparent solubility product from the experimental data (Table VIII-3, Jang, 2022) and that calculated from the EQ3NR model response were graphically compared. The results are plotted in Figure 7, and the method used to calculate the apparent log K is presented below.

The dissolution reaction for abellaite can be written as:

$$NaPb_2(CO_3)_2(OH) + 3H^+ \rightleftharpoons 2Pb^{2+} + Na^+ + 2HCO_3^- + H_2O$$

The apparent solubility product, Ksp,app, for the dissolution of abellaite follows:

$$Ksp,app = \{[Pb^{2+}]^2 \times [Na^+] \times [HCO_3^-]^2\} / [H^+]^3$$

By definition, the activity of a pure solid is equal to 1. The activity of water is set here to be equal to 1 for simplicity of calculation of Ksp,app. Note the square brackets ([-]) indicate concentration in units of molality (m). The log of the apparent solubility product is then given by:

$$\log Ksp,app = 2\log[Pb^{2+}] + \log[Na^+] + 2\log[HCO_3^-] + 3pmH$$

Table 5 provides the pmH, Na, Pb, and bicarbonate molality values used to calculate the log Ksp,app values for abellaite for the experimental and simulated values.

Table 5. Apparent Log K Values for Abellaite.

Table VIII-1 (Jang, 2022)					EQ3NR Simulated				
pmH	**Na (m)**	**Pb (m)**	**HCO_3^- (m)**	**log Ksp,app**	**pmH**	**Na (m)**	**Pb (m)**	**HCO_3^- (m)**	**log Ksp,app**
9.72	0.136	2.18E-05	8.47E-02	16.83	9.72	0.136	2.32E-05	8.47E-02	16.88
9.51	0.372	5.19E-05	2.57E-01	18.35	9.51	0.372	6.68E-05	2.57E-01	18.57
9.43	1.080	1.99E-04	6.76E-01	20.58	9.43	1.080	1.89E-04	6.76E-01	20.54
9.43	1.740	4.00E-04	1.03	21.76	9.43	1.740	3.10E-04	1.03	21.54
9.48	2.780	8.42E-04	1.51	23.09	9.48	2.780	6.65E-04	1.51	22.89
9.50	3.090	8.18E-04	1.69	23.27	9.50	3.090	9.71E-04	1.69	23.42

Information Only

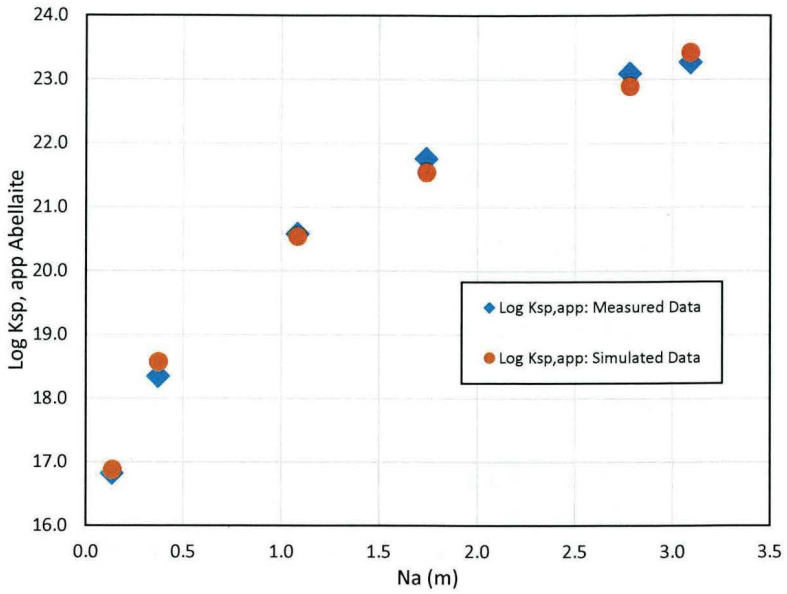


Figure 7. Apparent Log Ksp values for the abellaite measured data compared to the model predicted apparent Log Ksp values.

The apparent abellaite log Ksp values in Table 5 from the experiment and the model are plotted in Figure 7 for visual inspection.

Figures 6 and 7 demonstrate that the abellaite solubility product adequately reproduces the training data, i.e., the measured solubility data. This visual comparison of the abellaite solubility model to the experimental data shown in Figure 7 provides evidence that the model meets the acceptance criteria of AP-200 (Domski, 2022).

3.1.2 The Iron System

The iron system as presented by Kim et al. (2017) will be included in DATA0.FM6. Model parameters included in the new database were either derived by Kim et al. (2017), or originate in the literature. Tables 6 – 9 include the parameters that are included in DATA0.FM6 for the iron system. Inclusion of the Iron – Sulfate system (Jang, 2023b) in DATA0.FM6 addresses EPA Issue 32 (Peake, 2022).

Table 6. Equilibrium Constants for Reactions with Iron that will be included in DATA0.FM6

Reaction	log K	Source
Solid Dissolution Reactions		
$Fe(OH)_2(s) + 2H^+$ (ferrous hydroxide) $\rightleftharpoons Fe^{2+} + 2H_2O$	12.89	Kim et al. (2017)
$Fe_2Cl(OH)_3(s) + 3H^+$ (hibbingite) $\rightleftharpoons 2Fe^{2+} + Cl^- + 3H_2O$	17.08	Kim et al. (2017)
$FeCO_3(s) + H^+$ (siderite) $\rightleftharpoons Fe^{2+} + HCO_3^-$	-0.12	Stumm and Morgan (1996)
$Fe_2CO_3(OH)_2(s) + 3H^+$ (chukanovite) $\rightleftharpoons 2Fe^{2+} + HCO_3^- +$	12.32	Kim et al. (2017)

Information Only

$2H_2O$		
$FeSO_4.H_2O(s)$ (Szomolnokite) ⇌ $Fe^{2+} + SO4^{2-} + H_2O$	-0.90	Reardon and Beckie (1987)
$FeSO_4.7H_2O(s)$ (Melanterite) ⇌ $Fe^{2+} + SO4^{2-} + 7H_2O$	-2.20	Reardon and Beckie (1987)
Aqueous Dissociation Reactions		
$FeOH^+ + H^+ ⇌ Fe^{2+} + H_2O$	9.31	Shock et al. (1997)
$Fe(OH)_2(aq) + 2H^+ ⇌ Fe^{2+} + 2H_2O$	20.84	Lemire et al. (2013), Jang et al. (2021b)
$Fe(OH)_3^- + 3H^+ ⇌ Fe^{2+} + 3H_2O$	31.0	Baes and Mesmer (1976)
$Fe(OH)_4^{2-} + 4H^+ ⇌ Fe^{2+} + 4H_2O$	46.00	Baes and Mesmer (1976)
$FeCO_3(aq) + H^+ ⇌ Fe^{2+} + HCO_3^-$	4.83	Bruno et al. (1992)
$Fe(CO_3)_2^{2-} + 2H^+ ⇌ Fe^{2+} + 2HCO_3^-$	13.89	Kim et al. (2017)
$FeEDTA^{2-} ⇌ Fe^{2+} + EDTA^{4-}$	-16.1	Morel and Hering (1993)
$FeCitrate^- ⇌ Fe^{2+} + Citrate^{3-}$	-5.7	Morel and Hering (1993)
$FeOHCitrate^{2-} + H^+ ⇌ Fe^{2+} + Citrate^{3-} + H_2O$	2.24	Jang et al. (2021b)

Table 7. Pitzer Interaction Coefficients (Cation-Anion Interactions) for Ions Containing Iron that will be included in DATA0.FM6

I	*j*	α_1/α_2	$\beta^{(0)}$	$\beta^{(1)}$	$\beta^{(2)}$	C^{φ}	Source
Fe^{2+}	Cl^-	2.0/12.0	0.37324	1.13499	0.0	-0.02152	Moog et al. (2004)
Na^+	$Fe(CO_3)_2^{2-}$	2.0/12.0	-0.230	6.26	0.0	0.0	Kim et al. (2017)
Fe^{2+}	SO_4^{2-}	1.4/12.0	0.2568	3.063	-42.0	0.0209	Reardon and Beckie (1987)
Fe^{2+}	HSO_4^-	2.0/12.0	0.4273	3.48	0.0	0.0	Reardon and Beckie (1987)

Table 8. Pitzer Interaction Coefficients (Cation-Cation Interactions) for Ions Containing Iron that will be included in DATA0.FM6

i	*j*	θ_{ij}	Source
Na^+	Fe^{2+}	0.10945	Moog et al. (2004)
Mg^{2+}	Fe^{2+}	0.14504	Moog et al. (2004)

Table 9. Pitzer Interaction Coefficients (Cation-Cation-Anion Interactions) for Ions Containing Iron that will be included in DATA0.FM6

I	*j*	*k*	ψ_{ijk}	Source
Fe^{2+}	Na^+	Cl^-	-0.01605	Moog et al. (2004)

Information Only

Fe^{2+}	Mg^{2+}	Cl^-	-0.02985	Moog et al. (2004)
Fe^{2+}	HSO_4^-	Cl^-	0.0143	Reardon and Beckie (1987)

To demonstrate the adequacy of the solubility products of the iron solid phases hibbingite, $Fe(OH)_2(s)$, and chukanovite, of Kim et al. (2017) their respective apparent solubility products based on the experimental data (Tables 1 and 5, Kim et al. 2017) and the EQ3NR model response were calculated and tabulated. The results are plotted in Figure 8 - 10, and the method used to calculate the apparent log K values is presented below.

The apparent solubility product, log Ksp,app, for the dissolution of hibbingite, ferrous Hydroxide, and chukanovite was calculated as follows:

The dissolution reaction for hibbingite can be written as:
$Fe_2Cl(OH)_3(s) + 3H^+ \rightleftharpoons 2Fe^{2+} + Cl^- + 3H_2O$

The apparent solubility product is given by:

$Ksp,app = \{[Fe^{2+}]^2 \times [Cl-]\} / [H^+]^3$

The log of the apparent solubility product is given by:

$\log Ksp,app = 2\log[Fe^{2+}] + \log[Cl^-] + 3pmH$

The dissolution reaction for ferrous hydroxide can be written as:

$Fe(OH)_2(s) + 2H^+ \rightleftharpoons Fe^{2+} + 2H_2O$

The apparent solubility product is given by:

$Ksp,app = [Fe^{2+}] / [H^+]^2$

The log of the apparent solubility product is given by:

$\log Ksp,app = \log[Fe^{2+}] + 2pmH$

The dissolution reaction for chukanovite can be written as:

$Fe_2CO_3(OH)_2(s) + 3H^+ \rightleftharpoons 2Fe^{2+} + HCO_3^- + 2H_2O$

The apparent solubility product is given by:

$Ksp,app = \{[Fe^{2+}]^2 \times [HCO_3^-]\} / [H^+]^3$

The log of the apparent solubility product is given by:

Information Only

$$\log K_{sp,app} = 2\log[Fe^{2+}] + \log[HCO_3^-] + 3pmH$$

By definition, the activity of a pure solid is equal to 1. The activity of water is set equal to 1 for simplicity of calculation of Ksp,app. Note the square brackets ([-]) indicate concentration in units of molality (m).

Table 10 provides the NaCl, Fe, and pmH values used to calculate the $\log_{10}$ Ksp,app values for hibbingite as a function of NaCl concentration for the experimental and simulated values. The log Ksp,app values are plotted in Figure 8.

Table 10. Apparent Log Ksp values for Hibbingite.

Measured Data from Table 1 Kim et al. (2017)				EQ3NR Simulated Data			
NaCl (m)	**Fe (m)**	**pmH**	**logKsp,app**	**NaCl (m)**	**Fe (m)**	**pmH**	**logKsp,app**
0.1	1.40E-03	8.21	17.92	0.1	1.31E-03	8.21	17.86
1.0	3.23E-04	8.52	18.58	1.0	3.32E-04	8.52	18.60
2.0	2.71E-04	8.57	18.88	2.0	2.63E-04	8.57	18.85
3.0	2.08E-04	8.64	19.03	3.0	2.04E-04	8.64	19.02
4.0	1.61E-04	8.71	19.15	4.0	1.66E-04	8.71	19.17
5.0	1.63E-04	8.72	19.28	5.0	1.69E-04	8.72	19.31

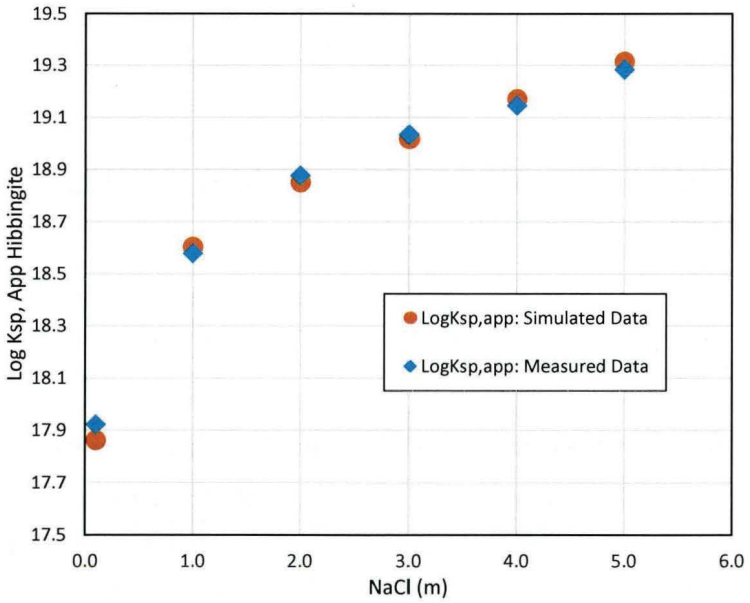


Figure 8. Apparent log Ksp values for the hibbingite measured data compared to the model predicted apparent log Ksp values.

Table 11 provides the NaCl, Fe, and pmH values used to calculate the log Ksp,app values for ferrous hydroxide as a function of NaCl concentration for the experimental and simulated values. The log Ksp,app values are plotted in Figure 9.

Table 11. Apparent Log Ksp values for Ferrous Hydroxide.

Information Only

Measured Data Table 1 Kim et al. (2017)				EQ3NR Simulated Data			
NaCl (m)	Fe (m)	pmH	logKsp,app	NaCl (m)	Fe (m)	pmH	logKsp,app
0.04	1.49E-03	7.94	13.05	0.04	1.62E-03	7.94	13.09
0.15	1.19E-03	8.04	13.16	0.15	1.36E-03	8.04	13.21
0.50	1.08E-03	8.15	13.33	0.50	1.22E-03	8.15	13.38
1.22	9.14E-04	8.29	13.54	1.22	9.81E-04	8.29	13.57
3.03	6.82E-04	8.48	13.79	3.03	8.75E-04	8.48	13.90

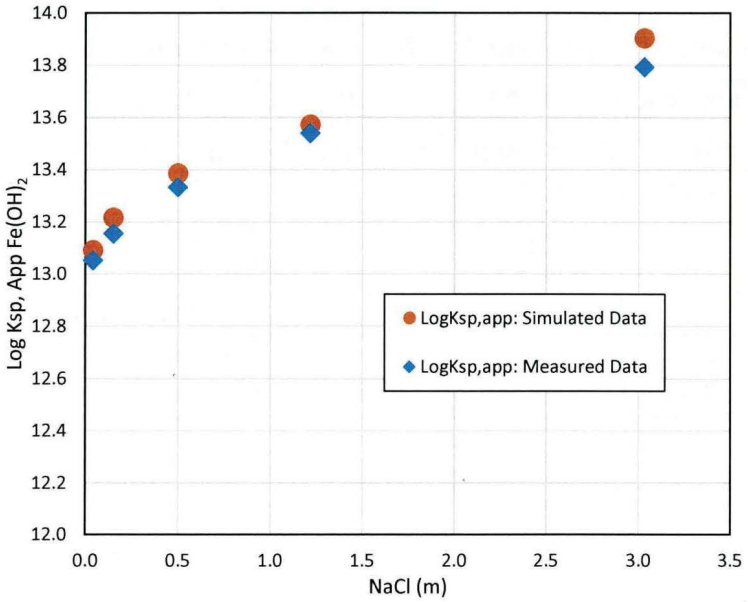


Figure 9. Apparent log Ksp values for the ferrous hydroxide measured data compared to the model predicted apparent log Ksp values.

Table 12 provides the Na, Cl, Fe, HCO_3, and pmH values used to calculate the log Ksp,app values for chukanovite as a function of sodium concentration for the experimental and simulated values. The log Ksp,app values are plotted in Figure 10.

Table 12. Apparent Log Ksp values for Chukanovite.

Measured Data, Table 5 Kim et al. (2017)						EQ3NR Simulated Data					
HCO_3 (m)	Fe (m)	Na (m)	Cl (m)	pmH	logKsp, app	HCO_3 (m)	Fe (m)	Na (m)	Cl (m)	pmH	logKsp, app
2.0	2.53E-04	4.15	0.15	10.56	24.79	2.0	1.65E-04	4.15	0.15	10.56	24.42
0.5	1.91E-05	2.50	1.50	10.41	21.49	0.5	3.06E-05	2.50	1.50	10.41	21.90
1.0	4.98E-05	3.50	1.50	10.42	22.65	1.0	8.36E-05	3.50	1.50	10.42	23.10
1.5	1.06E-04	4.50	1.50	10.65	24.18	1.5	1.49E-04	4.50	1.50	10.65	24.47
2.0	1.98E-04	5.50	1.50	10.64	24.81	2.0	4.54E-04	5.50	1.50	10.64	25.53
0.5	1.37E-05	1.15	0.15	10.38	21.11	0.5	2.75E-05	1.15	0.15	10.38	21.72
1.0	5.86E-05	2.15	0.15	10.32	22.50	1.0	5.54E-05	2.15	0.15	10.32	22.45
1.5	1.31E-04	3.15	0.15	10.38	23.55	1.5	1.03E-04	3.15	0.15	10.38	23.34

Information Only

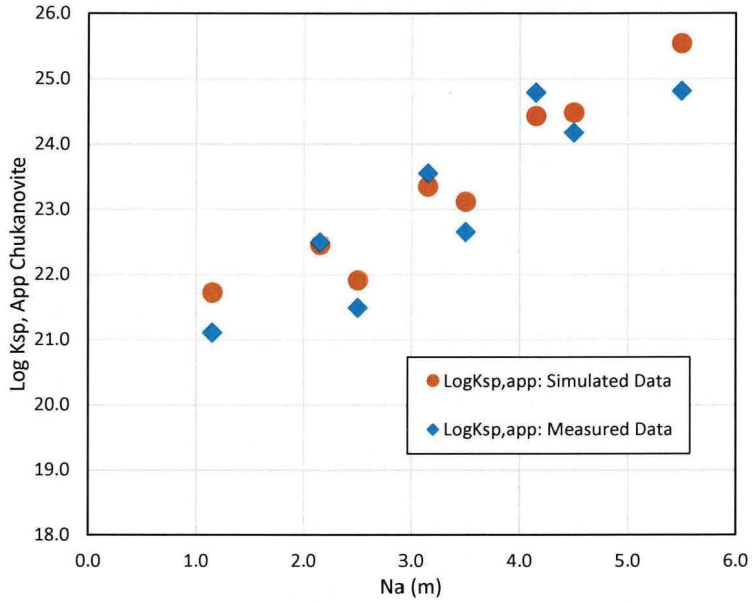


Figure 10. Apparent log Ksp values for the chukanovite measured data compared to the model predicted apparent log Ksp values.

It is the authors' opinion that Figures 8 – 10 show that the model response provides an adequate fit to the measured data. Thus, Figures 8 – 10 provide evidence that the iron-phase models of Kim et al. (2017) meet the acceptance criteria of AP-200 (Domski, 2022).

3.1.3 Magnesium Model

Jang (2020) and Jang et al. (2020) considered the $MgOxalate{\cdot}2H_2O(s)$ – $Na_2Oxalate$ – H_2O system. Glushinskite ($MgOxalate{\cdot}2H_2O(s)$) was added to solution containing increasing concentrations of $Na_2Oxalate$. The goal of this study was to accurately model how the common-ion effect ($Oxalate^{2-}$ in this case) impacts the solubility of Glushinskite ($MgOxalate \cdot 2H_2O(s)$). To describe the behavior of ΣMg as a function of the $\Sigma Na_2Oxalate$ loading, Jang et al. (2021b) used the complexation constant of $Mg(Oxalate)_2^{2-}$ from Martell and Smith (1977) (log K = -4.94) and the solubility constant of $MgOxalate{\cdot}2H_2O(s)$ from Hummel et al. (2005) (log K = -6.4 ±0.2). However, the model overestimated the maximum uncertainty associated with ΣMg over the entire range (Jang et al., 2021b), this was attributed to slow kinetics of solubility equilibrium of $MgOxalate{\cdot}2H_2O(s)$ (Hummel et al., 2005). The fit was achieved within the measurement uncertainties only when adjusting the log K of Glushinskite ($MgOxalate \cdot 2H_2O(s)$) to -6.49, as shown in Figure 11. Jang (2020) aged their experiment for more than 800 days to address the slow kinetics of solubility equilibrium proposed in Hummel et al. (2005), which corroborates the log K closer to the lower end of the range given in Hummel et al. (2005). The new recommended log K values to be added to FM6 are summarized in Table 13.

Information Only

Table 13. Reactions and log K values at 25 °C and I = 0 used for the Mg-Oxalate system.

Reaction	log K	Source
Solid Dissolution Reactions		
$MgOxalate{\cdot}2H_2O(s)$ (Glushinskite) ⇌ Mg^{2+} + $Oxalate^{2-}$ + 2H2O	-6.49	Jang et al. (2021b)
Aqueous Dissociation Reactions		
$Mg(Oxalate)_2^{2-}$ ⇌ Mg^{2+} + 2$Oxalate^{2-}$	-4.94	Martell and Smith (1977)

Jang et al. (2021b) included the Mg – Oxalate aqueous species $Mg(Oxalate)_2^{2-}$ of Martell and Smith (1977) to fit the solubility product of Glushinskite, no additional Pitzer parameters were required. Figures 10 and 11 show the Glushinskite model-calibration adequacy, showing the model response compared to the measured magnesium and sodium training data, and the apparent solubility products versus the sodium concentration, respectively.

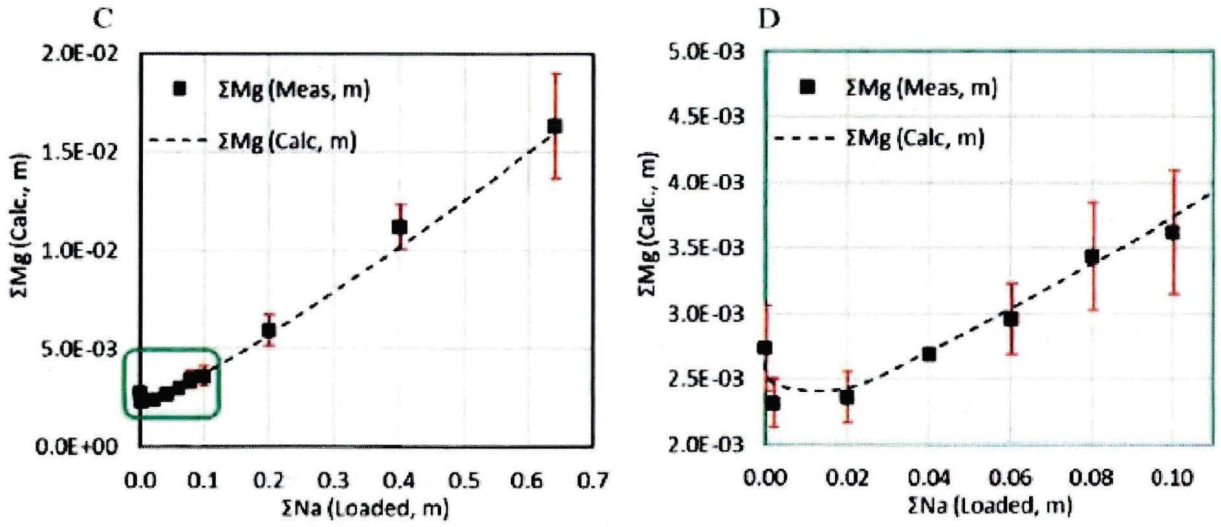


Figure 11. Reproduction of Figure VI.1-10, parts C and D from Jang et al. (2021b). Parametrization of $MgOxalate{\cdot}2H_2O(s)$ – $Na_2Oxalate$ – H_2O system. Fitting of the model using the new recommended glushkinskite log Ksp. B is a zoomed-in view of the green rectangle in A.

To build additional confidence in the glushinskite solubility product its apparent solubility product based on the experimental data (Table VI.1-10, Jang et al., 2021b) and the EQ3NR model response was calculated. The results are plotted in Figure 12, and the method used to calculate the apparent log K is presented below.

The dissolution reaction for glushinskite can be written as:

$Mg(Oxalate)_2^{2-}$ ⇌ Mg^{2+} + 2$Oxalate^{2-}$

The apparent solubility product is given by:

Information Only

$Ksp,app = [Mg^{2+}] / [Oxalate^{2-}]^2$

By definition, the activity of a pure solid is equal to 1. The activity of water is purposely set equal to 1 for simplicity of calculation of Ksp,app. Note the square brackets ([-]) indicate concentration in units of molality (m).

The $\log_{10}$ of the apparent solubility product is then given by

$\log Ksp,app = \log [Mg^{2+}] + 2\log[Oxalate^{2-}]$

Table 14 provides the pmH, Mg, Na, and oxalate molalities used to calculate the log Ksp,app values for glushinskite as a function of sodium concentration for the experimental and simulated values.

Table 14. Apparent Log K values for Glushinskite.

Measured Data from Jang et al. (2021b), Table VI.1-10					**EQ3NR Simulated Data**				
pmH	**Mg (m)**	**Na (m)**	**Oxalate (m)**	**logKsp,app**	**pmH**	**Mg (m)**	**Na (m)**	**Oxalate (m)**	**logKsp,app**
8.34	2.74E-03	5.36E-04	5.33E-03	-7.11	8.34	2.35E-03	5.36E-03	5.03E-03	-7.23
8.31	2.32E-03	4.07E-03	2.56E-03	-7.82	8.31	2.38E-03	4.07E-03	4.41E-03	-7.33
8.13	2.36E-03	1.98E-02	9.27E-03	-6.69	8.13	2.44E-03	1.98E-02	1.23E-02	-6.43
8.19	2.69E-03	6.65E-02	2.15E-02	-5.91	8.19	3.16E-03	6.65E-02	3.64E-02	-5.38
8.26	2.96E-03	8.29E-02	3.19E-02	-5.52	8.26	3.44E-03	8.29E-02	4.49E-02	-5.16
8.27	3.43E-03	1.00E-01	4.21E-02	-5.22	8.27	4.11E-03	1.19E-01	6.36E-02	-4.78
8.29	3.62E-03	1.19E-01	5.21E-02	-5.01	8.29	6.15E-03	2.20E-01	1.16E-01	-4.08
8.37	5.94E-03	2.20E-01	1.04E-01	-4.19	8.37	1.04E-02	4.09E-01	2.15E-01	-3.32
8.49	1.11E-02	4.09E-01	2.27E-01	-3.24	8.49	1.35E-02	5.37E-01	2.82E-01	-2.97
8.59	1.63E-02	5.37E-01	2.61E-01	-2.95	8.59	1.35E-02	5.38E-01	2.82E-01	-2.97

Information Only

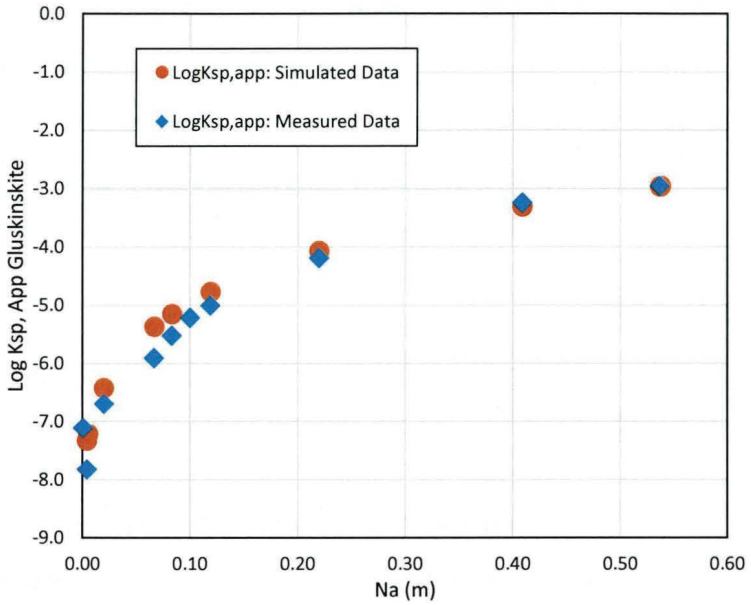


Figure 12. Apparent Log Ksp values for the glushinskite measured data compared to the model predicted apparent Log Ksp values.

Figures 11 and 12 show the training-data-model comparison, thus the magnesium – oxalate model for the solubility of glushinskite is considered acceptable via the acceptance criteria of AP-200 (Domski, 2022).

3.1.4 Earlandite Solubility Product

In their completeness comment CC2-GEOCHEM-13, and EPA Issue 29 (Peake, 2022) for Compliance Recertification Application - 2019 Deferred Performance Assessment (CRA-2019 DPA) the EPA noted that the solubility product for earlandite ($Ca_3(Citrate)_2 \cdot 4H_2O$) was omitted contrary to the analysis plan, AP-183, Rev.1, for DATA0.FM4 (Sisk-Scott, 2019). The omission of the solubility product of earlandite by the DOE was an oversight that will be corrected in DATA0.FM6. In response to the EPA's completeness comment, the DOE (Knerr, 2020) demonstrated that the absence of earlandite did not have any effect on the actinide baseline solubility predictions of Domski and Sisk-Scott (2019) for the CRA-2019 DPA. The solubility product for earlandite is presented in Table 15.

Table 15. Solubility constant of Earlandite ($Ca_3(Citrate)_2 \cdot 4H_2O$) to be implemented in DATA0.FM6.

Reaction	log K	Source
Solid Dissolution Reactions		
$Ca_3(Citrate)_2 \cdot 4H_2O \rightleftharpoons 3Ca^{2+} + 2Citrate^{3-} + 4H_2O$	-17.9	Hummel et al. (2005)

3.1.5 An(III) Model

Information Only

Jang et al. (2021b) tested if the current An(III) model used in DATA0.FM1 would accurately predict the solubility of $Nd(OH)_3(s)$ as a function of incremental $MgCl_2$ ($Nd(OH)_3(s)$ - $MgCl_2$ - H_2O system). Model parametrization was performed using the solubility constant log K(Nd(OH)3(s)) = 16.9 (Guillaumont et al., 2003) along with an updated Pitzer interaction parameter (PIP) ($Nd(OH)_2^+/Mg^{2+}$) = 0.302 (Figure 13). Log K = 16.9 (Guillaumont et al., 2003) was chosen over log K = 14.49 (DATA0.FM1) and log K = 15.6, because it resulted in saturation indices closest to 0 calculated from the data in Table VII.1-10 (Jang et al., 2021b) . The recommended values are summarized in Table 16.

Table 16. Recommendation of new Pitzer parameters for the $Nd(OH)_3(s)$ - $MgCl_2$ - H_2O system. Note: Nd(III) is an analog for Am(III).

Reaction		log K	Source
Solid Dissolution Reactions			
$Am(OH)_3(am) + 3H^+ \rightleftharpoons Am^{3+} + 3H_2O$		16.9	Guillaumont et al. (2003)
i	***j***	**θ*ij***	**Source**
$Am(OH)_2^+$	Mg^{2+}	0.302	Jang et al. (2021b)

Figure 13 shows the model fit compared to measured solubility data of $Nd(OH)_3(am)$ in $MgCl_2$ solutions. Figure 12 demonstrates model-calibration adequacy using the $\log_{10}$ Ksp for $Nd(OH)_3(am)$ from Guillaumont et al. (2003) and using the cation – cation Pitzer parameter, θ, as the fitting parameter for the $Nd(OH)_2^+/Mg^{2+}$ pair.

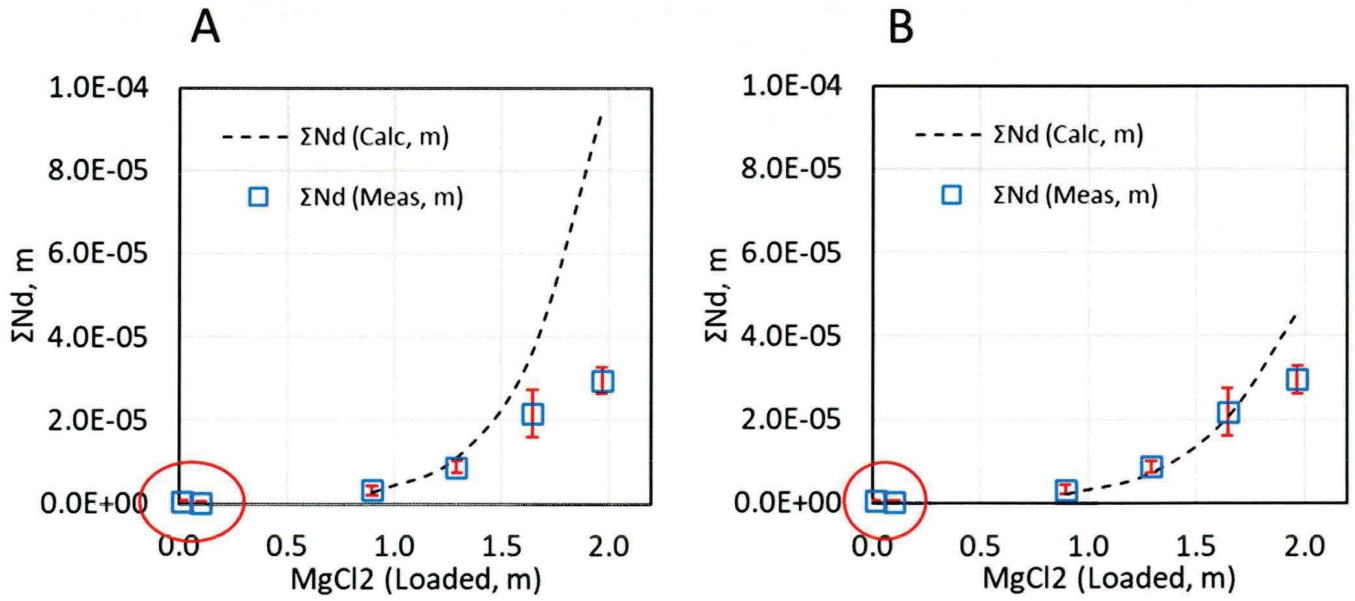


Figure 13. Model predictions of $Nd(OH)_3(s)$ – $MgCl_2$ – H_2O system reproduced from Figure VII.1-10 of, Jang et al. (2021b). Figure A: before fitting with updated PIP; and Figure B: after fitting with the updated in PIP.

Information Only

Confidence in the $Nd(OH)_3(am)$ solubility product was increased with calculation of its apparent solubility product from the experimental data (Table VII.1-10, Jang et al., 2021b) and the EQ3NR model response. The results are plotted in Figure 14, and the method used to calculate the apparent log K is presented below.

The dissolution reaction for $Am(OH)_3(am)$ can be written as:

$$Am(OH)_3(am) + 3H^+ \rightleftharpoons Am^{3+} + 3H_2O$$

The apparent solubility product is then given by:

$$K_{sp,app} = [Am^{3+}] / [H^+]^3$$

By definition, the activity of a pure solid is equal to 1. The activity of water is purposely set equal to 1 for simplicity of calculation of Ksp,app. Note the square brackets ([-]) indicate concentration in units of molality (m).

$$\log K_{sp,app} = \log [Am^{3+}] + 3pmH$$

Table 17 provides the pmH, and An(III) molalities used to calculate the log Ksp,app values for $Am(OH)_3(am)$ as a function of $MgCl_2$ concentration for the experimental and simulated values.

Table 17. Apparent Log K values for $Am(OH)_3(am)$.

Table VII.1-10 (Jang et al., 2021b)				EQ3NR Simulated		
Mg (m)	**pmH**	**Nd(III) (m)**	**log Ksp, app**	**pmH**	**Am(III) (m)**	**log Ksp, app**
0.895	8.39	3.26E-06	19.68	8.39	2.04E-06	19.48
1.29	8.29	8.76E-06	19.81	8.29	7.08E-06	19.72
1.64	8.20	2.18E-05	19.94	8.20	2.04E-05	19.91
1.97	8.15	2.96E-05	19.92	8.15	4.57E-05	20.11

Information Only

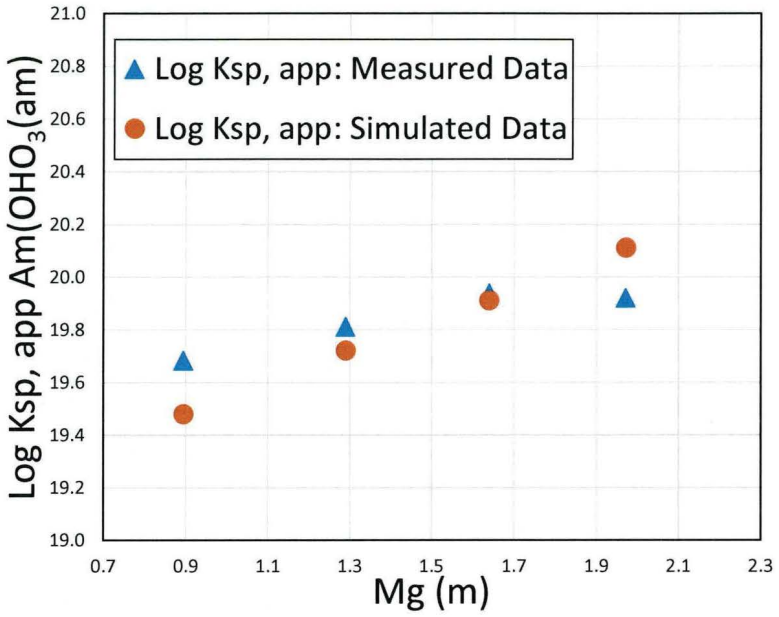


Figure 14. Apparent solubility product values for $Nd(OH)_3(am)$ from the experimental data of Jang et al. (2021b) and the model predicted values.

Figures 13 and 14 show that the model response provides an adequate fit to the measured data, thus, the An(III) model for the solubility of $Nd(OH)_3(am)$ is considered verified within the acceptance criteria of AP-200 (Domski, 2022).

3.2 Comparison of the Documented and DATA0.FM6 Fitted Parameters

Parameters that were estimated with the Python script of Kirchner (2012) were done so using a copy of DATA0.FM1 that included the addition of those fitting parameters and any supporting parameters. Thus, this interim database was specific to those parameters being fit, and differed from DATA0.FM6 which includes all of the new chemical systems outlined in this analysis report. Therefore, it was necessary to test DATA0.FM6 to ensure that it could reproduce the parameter values originally estimated using the interim database.

To test the ability of DATA0.FM6 to reproduce the fitted parameter values estimated using the Python script of Kirchner (2012) each script was executed using DATA0.FM6 and the results compared to the values documented in the references. A comparison of the derived parameters using the updated database with those tabulated above are shown in Table 18. The following procedure was followed:

1) Run the parameter fitting Python scripts using DATA0.FM6 for each of the fitted parameters as listed in the previous sections.
2) Compare the results with those documented in the analysis reports, and memos, i.e., the original derived parameter values. The original derived values (documented value) were accepted if the results of fitting with DATA0.FM6 were within 10% of the value (see AP-176, Revision 0, [Jang and Domski, 2017] Section 2.4 for the method of calculating the

Information Only

percent difference). It was expected that there would be some deviation between the original derived values and those derived with DATA0.FM6 because of the necessity of deriving the parameters in a stepwise fashion. Note that the 10% acceptance criterion is a conservative value based on the reproducibility of standards for the analytical equipment used to measure concentrations in the laboratory which have a 10% to 20% reproducibility range for check samples (standards), for example see SP 12-2, Revision 3, SP 12-9, Revision 5, SP 12-22, Revision 4. Since the derived parameters use the analytical data it would be expected there could be downstream error propagation which could result in even greater differences in the derived parameter reproducibility, therefore, the 10% percent acceptance criteria is justified and conservative.

3) If the difference in the fitted parameter values using DATA0.FM6 was greater than 10%, then the appropriate analysis report, or memo, was updated to reflect the new parameters and DATA0.FM6 was also updated to reflect these changes.

A comparison of the derived parameters using the updated database with those tabulated above are shown in Table 18.

Table 18. Comparison of the documented parameters with those estimated using DATA0.FM6

Chemical Entity	Fitting Parameter	Documented Value	Estimated with DATA0.FM6	Comments
Abellaite [$NaPb_2(CO_3)_2(OH)$]	Log K	2.59	2.599	The lead parameters are all identical. Note, Jang (2022) fit values were identical to those estimated with DATA0.FM6, but Jang chose to truncate the values at the second decimal place for the log K values, and third decimal for the θ value.
$Pb(CO_3)_3^{4-}$	Log K	27.19	27.192	
$PbCl_3^- / Na^+$	$\beta^{(0)}$	-0.10025	-0.10025	
$PbCl_3^- / Mg^{2+}$	$\beta^{(0)}$	0.23	0.23	
Pb^{2+} / H^+	θ	0.343	0.34375	
$PbCl_3^- / H^+$	$\beta^{(0)}$	0.1077	0.1077	
	$\beta^{(1)}$	0.0425	0.0425	
	$\beta^{(2)}$	0.0	0.0	
	$C\phi$	-0.0035	-0.0035	
Glushinskite [$MgOxalate \cdot 2H_2O(s)$]	Log K	-6.49	-6.49	Values are identical
$Am(OH)_2^+ / Mg^{2+}$	θ	0.302	0.302	Values are identical
$FeOHCitrate^{2-}$	Log K	2.24	2.24	Values are identical

The results of running the parameter fitting scripts using DATA0.FM6 are tabulated above in Table 18, and the results show there were no differences between the documented values and those fit using DATA0.FM6. Therefore, the results meet the acceptance criteria of AP-200 (Domski, 2022).

Information Only

4 CONCLUSIONS

The objective of this analysis report is to document the addition of parameters to a current quality assured WIPP EQ3/6 thermodynamic database, DATA0.FM1 (Xiong, 2011), to create a new WIPP EQ3/6 model-parameter database, DATA0.FM6. This new database is intended to be used for calculating actinide solubility values for the Replacement Panels Planned Change Request (RPPCR) and the 2024 Compliance Recertification Application (CRA-2024).

The new WIPP database, DATA0.FM6, replaces the WIPP database used for the CRA-2019 DPA, DATA0.FM4 (Domski, 2019), and its update, DATA0.FM5 (Domski, 2020). During the completeness process for the CRA-2019 DPA the EPA had four issues 5, 8, 29, and 32 (Peake, 2022) which are directly addressed with the issuing of DATA0.FM6, these include: 1) EPA Issue 5, the DATA0.FM4 EDTA model; 2) EPA Issue 8, removal and replacement of the FM4/FM5 lead model with a Pitzer based lead model; 3) Issue 29, inclusion of the calcium citrate solid phase Earlandite; and 4) Issue 32, inclusion of the iron – sulfate model. In addition to these four changes in DATA0.FM6 there was also the addition of the Nd(III) hydroxide amorphous solid phase log K value to represent $Am(OH)_3(am)$, the inclusion of iron organic ligand complexes with EDTA and citrate, and an update to the magnesium – oxalate system including the Mg-oxalate solid phase glushinskite. These updates seek to prioritize impacts on actinide solubility and near-field geochemistry. The primary focus of the current updates are improvements to the chemical models of the waste and waste packaging that have large inventories, in this case iron and lead. Demonstration of the fit of the new chemical systems was accomplished in their source documentation, reproduced here, and by comparison of the experimental and simulated apparent, or conditional solubility constants for important solid phases.

Information Only

5 REFERENCES

Activity/Project Specific Procedure, SP 12-2, Use and Maintenance of the UIC, INC. Model CM5015 CO2 Coulometer, CM5130 Acidification Module, CM5300 Furnace Apparatus and CM5390 Automated Boat Inlet, Revision 3. April 28, 2011. Carlsbad, NM: Sandia National Laboratories.

Activity/Project Specific Procedure, SP 12-9, Calibration, use, and Maintenance of the Perkin Elmer Optima 8300 Dual View (DV) Inductively Coupled Plasma Atomic Emission Spectroscopy (ICP-AES) Revision 5. August 29, 2017. Carlsbad, NM: Sandia National Laboratories.

Activity/Project Specific Procedure, SP 12-22, Calibration, Use, and Maintenance of the Dionex Ion Chromatograph (IC) 6000. October 31, 2019. Carlsbad, NM: Sandia National Laboratories.

Baes, C. F.; Mesmer, R. E. 1976. The Hydrolysis of Cations. Wiley Interscience: New York.

Bruno, J.; Wersin, P.; Stumm, W. Stumm, W. On the Influence of Carbonate in Mineral Dissolution: II. The Solubility of FeCO3(s) at 25 °C and 1 atm total pressure. Geochim. Cosmochim. Acta 1992, 56, 1149−1155.

Domski, P. and C. Sisk-Scott. 2019. Prediction of Baseline Actinide Solubilities for CRA 2019 with and Updated EQ3/6 Pitzer Thermodynamic Database, DATA0.FM4. Carlsbad, NM: Sandia National Laboratories. ERMS 571178

Domski, P.S. 2019. "Official Release of the Qualified Pitzer Thermodynamic Database, DATA0.FM4, for EQ3/6 under AP-183, Revision 1. Carlsbad, NM: Sandia National Laboratories. ERMS 571051.

Domski, P.S. 2020. DATA0.FM5: Official Release of the Qualified Pitzer Thermodynamic Database, DATA0.FM5, for EQ3/6 under AP-183, Revision 1. Carlsbad, NM: Sandia National Laboratories. ERMS 572791

Domski, P. 2022 "Analysis Plan: Procedure(s) for the Creation of Thermodynamic Databases for WIPP Compliance Calculations". AP-200. Carlsbad, NM: Sandia National Laboratories. ERMS 578657

Domski, P. 2023 "Memo of Correction: : Transcription Error of $\beta^{(0)}$ value for the Mg2+ - PbCl3- Binary Pitzer Parameter in GEOC 21-11". Carlsbad, NM: Sandia National Laboratories. ERMS PENDING.

Edwards, R., R. D. Gillard, P. A. Williams, and A. M. Pollard, 1992. Studies of secondary minerals formation in the PbO - H_2O - HCl system. Mineralogical Magazine, 56, 53-65.

Information Only

Guillaumont, R., Fanghänel, T., Fuger, J., Grenthe, I., Neck, V., Palmer, D. A., and Rand, M. H., 2003. Update on the chemical thermodynamics of uranium, neptunium, plutonium, americium and technetium. OECD-NEA, Elsevier, Amsterdam.

Harvie, C. E., N. Møller, and J. H. Weare, 1984. The prediction of mineral solubilities in natural waters: The Na-K-Mg-Ca-H-Cl-SO4-OH-HCO3-CO3-CO2-H2O system to high ionic strengths at 25°C. Geochimica et Cosmochimica Acta, 48, 723-751.

Hummel, W., Anderegg, G., Puigdomenech, I., Rao, L., Tochiyama, O. (2005). Chemical Thermodynamics of Compounds and Complexes of U, Np, Pu, Am, Tc, Zr, Ni and Se with Selected Organic Ligands. Chemical Thermodynamics, Volume 9, OECD Nuclear Energy Agency, Data Bank, Issy-les-Moulineaux, France, Elsevier B.B. Amsterdam, The Netherlands, p. 1088.

Jang, J-H. and P. Domski. 2017. "Analysis Plan for the Development of a Self-Consistent Extension of the WIPP Geochemical Thermodynamic Database that Includes Aqueous Ferrous Iron Chemistry". AP-176. Carlsbad, NM: Sandia National Laboratories. ERMS 566478.

Jang, J., 2020. Experimental Study of the Thermodynamic Equilibrium Constants for the Magnesium - Oxalate Systems using Pitzer Activity Model, Revision 0. GEOC-19-05. Sandia National Laboratories, Carlsbad, New Mexico, U.S.A. ERMS 573285.

Jang, J., 2021. Revisit to the Pitzer Geochemical Thermodynamic Model for the $PbCl_2$(s)-HCl-H_2O System. Sandia National Laboratories, Carlsbad, NM, USA. ERMS 575309.

Jang, J., P. Hora, L. Kirkes, C. Miller, and L. Zhang, 2021a. Analysis Plan for Analysis Reports documenting Solubility and Complexation of Iron, Lead, Magnesium, Neodymium, and Boron in WIPP-Relevant Brines under Test Plans 00-07, 06-03, 08-02, 10-01, 12-02, 14-03, 14-05, 16-02, 19-01, and 20-01. Analysis Plan AP-190 Revision 0. Sandia National Laboratories, Carlsbad, New Mexico, U.S.A. ERMS 575624.

Jang, J., P. Hora, L. Kirkes, C. Miller, and L. Zhang, 2021b. Analysis Report documenting Solubility and Complexation of Iron, Lead, Magnesium, Neodymium, and Boron in the WIPP-Relevant Brines under TPs 06-03, 08-02, 12-02, 14-03, 14-05, 16-02, 19-01, and 20-01. Revision 0. GEOC-21-11. Sandia National Laboratories, Carlsbad, New Mexico, U.S.A. ERMS 576381. SAND2022-13723R.

Jang, J., 2022. The PbCO3(s) - $NaHCO_3$ - Na_2CO_3 - H_2O Experiment (Revision 0): Addendum to Xiong (2015a,b). Memo to SNL WIPP Records Center and SNL WIPP Geochemistry. December 2, 2022. Sandia National Laboratories, Carlsbad, New Mexico, U.S.A. ERMS 578642.

Jang, J., and I. Foli, 2023a. Solubility and Complexation of Iron, Lead, Magnesium, Neodymium, Boron, and Calcium in Brines, Revision 1 of GEOC-21-11. GEOC-22-

Information Only

01/03/09. Sandia National Laboratories, Carlsbad, New Mexico. February 1, 2023. ERMS 578806.

Jang, J., 2023a. The $PbSO_4(s)$ - Na_2SO4 - NaCl - H_2O Experiment (Revision 0). Memo to SNL WIPP Records Center, SNL WIPP Geochemistry. January 30, 2023. Sandia National Laboratories, Carlsbad, New Mexico, U.S.A. ERMS 578721.

Jang, J., 2023b. Thermodynamic quantities for Fe^{+2} - SO_4^{-2} - H^+ - H_2O system (Revision 0). Memo to SNL WIPP Records Center, SNL WIPP Geochemistry. January 27, 2023. Sandia National Laboratories, Carlsbad, New Mexico, U.S.A. ERMS 578717.

Kim, S., C. Marrs, M. Nemer, and J-H. Jang 2017. "Solubility Model for Ferrous Iron Hydroxide, Hibbingite, Siderite, and Chukanovite in High Saline Solutions of Sodium Chloride, Sodium Sulfate, and Sodium Carbonate. Carlsbad, NM: Sandia National Laboratories. ERMS 569090.

Kirkes, L., T. Olivas, J. Jang, S. Kim, and Y. Xiong. 2014a. Third Milestone Report on Test Plan TP 08-02, "Iron, Lead, Sulfide, and EDTA Solubilities", Sandia National Laboratories, Carlsbad, New Mexico, U.S.A. ERMS 561911.

Kirkes, L., T. Olivas, J. Jang, S. Kim, and Y. Xiong. 2014b. Third Milestone Report on Test Plan TP 08-02, "Iron, Lead, Sulfide, and EDTA Solubilities", Revision 1, Sandia National Laboratories, Carlsbad, New Mexico, U.S.A. ERMS 562645.

Kirkes, L., T. Olivas, J. Jang, S. Kim, and Y. Xiong. 2014c. Third Milestone Report on Test Plan TP 08-02, "Iron, Lead, Sulfide, and EDTA Solubilities", Revision 2, Sandia National Laboratories, Carlsbad, New Mexico, U.S.A. ERMS 562947.

Kirchner, T.B., 2012. User's Manual for The EQ3CodeModule Version 1.00. Carlsbad, NM: Sandia National Laboratories. ERMS 557360.

Knerr, R. 2020. Response 6 to U.S. Environmental Protection Agency's 2019 Compliance Recertification Application Completeness Comments Letter dated March 23, 2020, May 8, 2020, June 12, 2020, and July 17, 2020 from Tom Peake to Mike Brown. U.S. Department of Energy, Carlsbad Field Office, Carlsbad, New Mexico. Letter to L.B. Veal, U.S. Environmental Protection Agency Radiation Protection Division, Washington, D.C. October 26, 2020.

Lemire, R. J.; Berner, U.; Musikas, C.; Palmer, D. A.; Taylor, P.; Tochiyama, O. Chemical Thermodynamics of Iron, Part 1. In Organisation for Economic Co-operation and Development; Perrone, J., Ed.; Nuclear Energy Agency, 2013; Vol. 13a, Chemical Thermodynamics.

Martell, A. E. and Smith, R. M., 1977. Critical Stability Constants. Volume 3: Other Organic Ligands. Plenum Press, New York.

Information Only

Miller, C., J. Jang, and I. Foli. 2023. Development of a WIPP Thermodynamic Database for Compliance Calculations. Memorandum to SNL WIPP Records. Carlsbad, NM: Sandia National Laboratories. ERMS: Pending

Millero, F. J. and Byrne, R. H., 1984. Use of Pitzer's equations to determine the media effect on the formation of lead chloro complexes. Geochimica et Cosmochimica Acta 48, 1145-1150.

Moog, H. C., Hagemann, S., and Rumyantsev, A. V., 2004. Isopiestic investigation of the systems FeCl2-(Na, K, Mg, Ca)Cl-H2O at 298.15 K. ZEITSCHRIFT FUR PHYSIKALISCHE CHEMIE-INTERNATIONAL JOURNAL OF RESEARCH IN PHYSICAL CHEMISTRY & CHEMICAL PHYSICS 218, 1063-1087.

Morel, F. M. M., and J. G. Hering, 1993. Principles and Applications of Aqueous Chemistry. John Wiley & Sons, Inc.

Nuclear Waste Management Procedure NP 9-1, Analyses. Revision 10. January 8, 2019. Carlsbad, NM: Sandia National Laboratories.

Peake, T. 2022. Letter to Michael Gerle "CRA-2019 Issues Table". U.S. Environmental Protection Agency, Center for Waste Management and Regulations. June 30, 2022.

Powell, K.J., Brown. P.L., Byrne, R.H., Gajda, T., Hefter. G., Luez, A.-K., Sjoberg, S., and Wanner, H., 2009. Chemical speciation of environmentally significant metals with inorganic ligands. Part 3: the Pb^{2+} + OH^-, Cl^-, CO_3^{2-}, SO_4^{2-}, and PO_4^{3-} systems (IUPAC Technical Report). Pure and Applied Chemistry 81 (12), 2425-2476

Reardon, E. J., and R. D. Beckie, 1987. Modelling chemical equilibria of acid mine-drainage: The $FeSO_4$-H_2SO_4-H_2O system. Geochimica et Cosmochimica Acta, 51, 2355-2368

Shock, E. L.; Sassani, D. C.; Willis, M. Sverjensky, D.A. 1997 Inorganic Species in Geologic Fluids: Correlations Among Standard Molal Thermodynamic Properties of Aqueous Ions and Hydroxide Complexes. Geochim. Cosmochim. Acta 1997, 61 (5), 907−950.

Sisk-Scott, C. 2019 "Analysis Plan to Update the WIPP Geochemical Thermodynamic Database (DATA0.FM1) to Data0.FM4 for CRA-2019". AP-183, Revision 1. Carlsbad, NM: Sandia National Laboratories. (ERMS# 571001).

Stumm, W.; Morgan, 1996. J. J. Aquatic Chemistry, 3rd ed.; John Wiley and Sons.

Xiong, Y.-L. 2011. "Release of EQ3/6 Database DATA0.FM1." E-mail to Jennifer Long, March 9, 2011. Carlsbad, NM: Sandia National Laboratories. ERMS 555152.

Xiong, Y.-L. 2015a. "Experimental and Thermodynamic Modeling Solubility of Cerussite, PbCO3(cr), in the Carbonate System to High Ionic Strengths, Revision 1, Supercedes ERMS 561917". Carlsbad, NM: Sandia National Laboratories. ERMS 564929.

Information Only

Xiong, Y.-L. 2015b. "Experimental Determination of Lead Carbonate Solubility at High Ionic Strengths: A Pitzer Model Description". Monateshefte fur Chemis, 146(9), 1433-1443.

Information Only

APPENDIX A. Updates and Additions to DATA0.FM1 to Create DATA0.FM6

Note: All references for the following parameter blocks are at the end of Appendix A.

```
+------------------------------------------------------------------------
elements
+------------------------------------------------------------------------
Fe         55.84500
Pb        207.19000
+------------------------------------------------------------------------
basis species
+------------------------------------------------------------------------
Fe++
     charge  =   2.0
****
     1 element(s):
      1.0000 Fe
****
+------------------------------------------------------------------------
Pb++
     charge  =   2.0
****
     1 element(s):
      1.0000 Pb
****
+------------------------------------------------------------------------
+------------------------------------------------------------------------
ca combinations: beta(n)(ca) and Cphi(ca) [optional: alpha(n)(ca)]
+------------------------------------------------------------------------
Na+                         Fe(CO3)2--
  alpha(1) = 2.0
  alpha(2) = 12.0
  beta(0)
    a1 = -0.230
    a2 = 0.
    a3 = 0.
    a4 = 0.
  beta(1)
    a1 = 6.26
    a2 = 0.
    a3 = 0.
    a4 = 0.
  beta(2)
    a1 = 0.
    a2 = 0.
    a3 = 0.
    a4 = 0.
  Cphi:
    a1 = 0.
    a2 = 0.
    a3 = 0.
    a4 = 0.
* Source: Kim et al (2017)
+------------------------------------------------------------------------
Fe++                        Cl-
  alpha(1) = 2.0
  alpha(2) = 12.0
  beta(0)
    a1 = 0.37324
```


Information Only

```
    a2 = 0.
    a3 = 0.
    a4 = 0.
  beta(1)
    a1 = 1.13499
    a2 = 0.
    a3 = 0.
    a4 = 0.
  beta(2)
    a1 = 0.
    a2 = 0.
    a3 = 0.
    a4 = 0.
  Cphi:
    a1 = -0.02152
    a2 = 0.
    a3 = 0.
    a4 = 0.
* Source: Moog et al. (2004)
+----------------------------------------------------------------
Fe++                          SO4--
  alpha(1) = 1.4
  alpha(2) = 12.0
  beta(0)
    a1 = 0.2568
    a2 = 0.
    a3 = 0.
    a4 = 0.
  beta(1)
    a1 = 3.063
    a2 = 0.
    a3 = 0.
    a4 = 0.
  beta(2)
    a1 = -42.0
    a2 = 0.
    a3 = 0.
    a4 = 0.
  Cphi:
    a1 = 0.0209
    a2 = 0.
    a3 = 0.
    a4 = 0.
* Source: Reardon and Beckie (1987)
+----------------------------------------------------------------
Fe++                          HSO4-
  alpha(1) = 2.0
  alpha(2) = 12.0
  beta(0)
    a1 = 0.4273
    a2 = 0.
    a3 = 0.
    a4 = 0.
  beta(1)
    a1 = 3.48
    a2 = 0.
    a3 = 0.
    a4 = 0.
  beta(2)
    a1 = 0.
    a2 = 0.
    a3 = 0.
    a4 = 0.
```


Information Only

```
  Cphi:
    a1 = 0.
    a2 = 0.
    a3 = 0.
    a4 = 0.
* Source: Reardon and Beckie (1987)
+-----------------------------------------------------------------
Na+                           PbCl3-
  alpha(1) = 2.0
  alpha(2) = 12.0
  beta(0)
    a1 = -0.10025
    a2 = 0.
    a3 = 0.
    a4 = 0.
  beta(1)
    a1 = 0.
    a2 = 0.
    a3 = 0.
    a4 = 0.
  beta(2)
    a1 = 0.
    a2 = 0.
    a3 = 0.
    a4 = 0.
  Cphi:
    a1 = 0.
    a2 = 0.
    a3 = 0.
    a4 = 0.
* Source: Jang et al (2021)
+-----------------------------------------------------------------
Mg++                          PbCl3-
  alpha(1) = 2.0
  alpha(2) = 12.0
  beta(0)
    a1 = 0.230125
    a2 = 0.
    a3 = 0.
    a4 = 0.
  beta(1)
    a1 = 0.
    a2 = 0.
    a3 = 0.
    a4 = 0.
  beta(2)
    a1 = 0.
    a2 = 0.
    a3 = 0.
    a4 = 0.
  Cphi:
    a1 = 0.
    a2 = 0.
    a3 = 0.
    a4 = 0.
* Source: Jang et al (2021)
+-----------------------------------------------------------------
H+                            PbCl3-
  alpha(1) = 2.0
  alpha(2) = 12.0
  beta(0)
    a1 = 0.1077
    a2 = 0.
```


Information Only

```
    a3 = 0.
    a4 = 0.
  beta(1)
    a1 = 0.0425
    a2 = 0.
    a3 = 0.
    a4 = 0.
  beta(2)
    a1 = 0.00
    a2 = 0.
    a3 = 0.
    a4 = 0.
  Cphi:
    a1 = -0.0035
    a2 = 0.
    a3 = 0.
    a4 = 0.0
* Source: Jang (2021)
+-----------------------------------------------------------------
*-----------------------------------------------------------------
* cc' combinations first, then aa' combinations
*-----------------------------------------------------------------
Na+                       Fe++
  theta:
    a1 = 0.10945
    a2 = 0.
    a3 = 0.
    a4 = 0.
* Source: Moog et al. (2004)
+-----------------------------------------------------------------
Mg++                      Fe++
  theta:
    a1 = 0.14504
    a2 = 0.
    a3 = 0.
    a4 = 0.
* Source: Moog et al. (2004)
+-----------------------------------------------------------------
Pb++                      H+
  theta:
    a1 = 0.343
    a2 = 0.
    a3 = 0.
    a4 = 0.
* Source: Jang and Foli (2023) from Jang (2023)
+-----------------------------------------------------------------
Am(OH)2+                  Mg++
  theta:
    a1 = 0.302
    a2 = 0.
    a3 = 0.
    a4 = 0.
* Source: Jang et al. (2021)
+-----------------------------------------------------------------
*-----------------------------------------------------------------
* cc'a combinations
*-----------------------------------------------------------------
Na+                       Fe++                      Cl-
  psi:
    a1 = -0.01605
    a2 = 0.
    a3 = 0.
    a4 = 0.
```


Information Only

```
* Source: Moog et al. (2004)
+------------------------------------------------------------
Mg++                      Fe++                      Cl-
  psi:
    a1 = -0.02985
    a2 = 0.
    a3 = 0.
    a4 = 0.
* Source: Moog et al. (2004)
+------------------------------------------------------------
Cl-                       Fe++                      HSO4-
  psi:
    a1 = 0.0143
    a2 = 0.
    a3 = 0.
    a4 = 0.
* Source: Reardon and Beckie (1987)
+------------------------------------------------------------
+------------------------------------------------------------------
aqueous species
+------------------------------------------------------------------
FeOH+                     FeOH+
     charge  =   1.0
****
     3 element(s):
      1.0000 H              1.0000 O              1.0000 Fe
****
     4 species in aqueous dissociation reaction:
    -1.0000  FeOH+                    -1.0000  H+
     1.0000  Fe++                      1.0000  H2O

**** logK grid [0-25-60-100C @1.0132bar; 150-200-250-300C @Psat-H2O]:
        No_Data    9.3100    No_Data    No_Data
        No_Data    No_Data    No_Data    No_Data
* Source: Shock et al. (1997)
+------------------------------------------------------------
Fe(OH)2(aq)               Fe(OH)2(aq)
     charge  =   0.0
****
     3 element(s):
      2.0000 H              2.0000 O              1.0000 Fe
****
     4 species in aqueous dissociation reaction:
    -1.0000  Fe(OH)2(aq)              -2.0000  H+
     1.0000  Fe++                      2.0000  H2O

**** logK grid [0-25-60-100C @1.0132bar; 150-200-250-300C @Psat-H2O]:
        No_Data   20.8400    No_Data    No_Data
        No_Data    No_Data    No_Data    No_Data
* Source: Lemire et al. (2013)
+------------------------------------------------------------
Fe(OH)3-                  Fe(OH)3-
     charge  =   -1.0
****
     3 element(s):
      3.0000 H              3.0000 O              1.0000 Fe
****
     4 species in aqueous dissociation reaction:
    -1.0000  Fe(OH)3-                 -3.0000  H+
     1.0000  Fe++                      3.0000  H2O

**** logK grid [0-25-60-100C @1.0132bar; 150-200-250-300C @Psat-H2O]:
        No_Data   31.0000    No_Data    No_Data
```


Information Only

```
        No_Data    No_Data    No_Data    No_Data
* Source: Baes and Mesmer (1976)
+---------------------------------------------------------------------
Fe(OH)4--                  Fe(OH)4--
     charge  =   -2.0
****
     3 element(s):
      4.0000 H               4.0000 O               1.0000 Fe
****
     4 species in aqueous dissociation reaction:
    -1.0000  Fe(OH)4--                -4.0000  H+
     1.0000  Fe++                      4.0000  H2O

**** logK grid [0-25-60-100C @1.0132bar; 150-200-250-300C @Psat-H2O]:
        No_Data    46.0000    No_Data    No_Data
        No_Data    No_Data    No_Data    No_Data
* Source: Baes and Mesmer (1976)
+---------------------------------------------------------------------
FeCO3                      FeCO3
     charge  =   0.0
****
     3 element(s):
      1.0000 C               3.0000 O               1.0000 Fe
****
     4 species in aqueous dissociation reaction:
    -1.0000  FeCO3                    -1.0000  H+
     1.0000  Fe++                      1.0000  HCO3-

**** logK grid [0-25-60-100C @1.0132bar; 150-200-250-300C @Psat-H2O]:
        No_Data    4.8300     No_Data    No_Data
        No_Data    No_Data    No_Data    No_Data
* Source: Bruno et al. (1992)
+---------------------------------------------------------------------
Fe(CO3)2--                 Fe(CO3)2--
     charge  =   -2.0
****
     3 element(s):
      2.0000 C               6.0000 O               1.0000 Fe
****
     4 species in aqueous dissociation reaction:
    -1.0000  Fe(CO3)2--               -2.0000  H+
     1.0000  Fe++                      2.0000  HCO3-

**** logK grid [0-25-60-100C @1.0132bar; 150-200-250-300C @Psat-H2O]:
        No_Data    13.8900    No_Data    No_Data
        No_Data    No_Data    No_Data    No_Data
* Source: Kim et al. (2017)
+---------------------------------------------------------------------
FeEDTA--                   FeC10H12O8N2--
     charge  =   -2.0
****
     5 element(s):
     10.0000 C              12.0000 H              1.0000 Fe
      2.0000 N               8.0000 O
****
     3 species in aqueous dissociation reaction:
    -1.0000  FeEDTA--                  1.0000  Fe++
     1.0000  EDTA----

**** logK grid [0-25-60-100C @1.0132bar; 150-200-250-300C @Psat-H2O]:
        No_Data   -16.1000    No_Data    No_Data
        No_Data    No_Data    No_Data    No_Data
* Source: Morel and Hering (1993)
```


Information Only

```
+---------------------------------------------------------------------
FeCitrate-                FeC6H5O7-
     charge  =   -1.0
****
     4 element(s):
      6.0000 C              5.0000 H              1.0000 Fe
      7.0000 O
****
     3 species in aqueous dissociation reaction:
    -1.0000  FeCitrate-               1.0000  Fe++
     1.0000  Citrate---

**** logK grid [0-25-60-100C @1.0132bar; 150-200-250-300C @Psat-H2O]:
        No_Data  -5.7000    No_Data   No_Data
        No_Data   No_Data   No_Data   No_Data
* Source: Morel and Hering (1993)
+---------------------------------------------------------------------
FeOHCitrate--             FeOHC6H5O7--
     charge  =   -2.0
****
     4 element(s):
      6.0000 C              6.0000 H              1.0000 Fe
      8.0000 O
****
     5 species in aqueous dissociation reaction:
    -1.0000  FeOHCitrate--            -1.0000 H+
     1.0000  Fe++                      1.0000  Citrate---
     1.0000  H2O
*
**** logK grid [0-25-60-100C @1.0132bar; 150-200-250-300C @Psat-H2O]:
        No_Data   2.2400    No_Data   No_Data
        No_Data   No_Data   No_Data   No_Data
* Source: Jang et al. (2021)
+---------------------------------------------------------------------
PbCl+                     PbCl+
     charge  =   1.0
****
     2 element(s):
      1.0000 Pb             1.0000 Cl
****
     3 species in aqueous dissociation reaction:
    -1.0000  PbCl+                        1.0000  Pb++
     1.0000  Cl-

**** logK grid [0-25-60-100C @1.0132bar; 150-200-250-300C @Psat-H2O]:
        No_Data   -1.4800   No_Data   No_Data
        No_Data   No_Data   No_Data   No_Data
* Source: Jang (2021), Millero and Byrne (1984)
+---------------------------------------------------------------------
PbCl2(aq)                 PbCl2(aq)
     charge  =   0.0
****
     2 element(s):
      1.0000 Pb             2.0000 Cl
****
     3 species in aqueous dissociation reaction:
    -1.0000  PbCl2(aq)                    1.0000  Pb++
     2.0000  Cl-

**** logK grid [0-25-60-100C @1.0132bar; 150-200-250-300C @Psat-H2O]:
        No_Data   -2.0300   No_Data   No_Data
        No_Data   No_Data   No_Data   No_Data
* Source: Jang (2021), Millero and Byrne (1984)
```


Information Only

```
+----------------------------------------------------------------
PbCl3-                    PbCl3(-)
     charge  =  -1.0
****
     2 element(s):
      1.0000 Pb             3.0000 Cl
****
     3 species in aqueous dissociation reaction:
    -1.0000  PbCl3-                      1.0000  Pb++
     3.0000  Cl-

**** logK grid [0-25-60-100C @1.0132bar; 150-200-250-300C @Psat-H2O]:
        No_Data   -1.8600  No_Data   No_Data
        No_Data   No_Data   No_Data   No_Data
* Source: Jang (2021), Millero and Byrne (1984)
+----------------------------------------------------------------
PbHCO3+                   PbHCO3+
     charge  =   1.0
****
     4 element(s):
      1.0000 Pb             1.0000 H             1.0000 C
      3.0000 O
****
     3 species in aqueous dissociation reaction:
    -1.0000  PbHCO3+                   1.0000  Pb++
     1.0000  HCO3-

**** logK grid [0-25-60-100C @1.0132bar; 150-200-250-300C @Psat-H2O]:
        No_Data  -1.8600    No_Data   No_Data
        No_Data   No_Data   No_Data   No_Data
* Source: Jang(2022)
+----------------------------------------------------------------
PbCO3(aq)                 PbCO3(aq)
     charge  =    0.0
****
     3 element(s):
      1.0000 Pb             1.0000 C             3.0000 O
****
     4 species in aqueous dissociation reaction:
    -1.0000  PbCO3(aq)                -1.0000  H+
     1.0000  Pb++                      1.0000  HCO3-

**** logK grid [0-25-60-100C @1.0132bar; 150-200-250-300C @Psat-H2O]:
        No_Data   3.8800    No_Data   No_Data
        No_Data   No_Data   No_Data   No_Data
* Source: Jang(2022)
+----------------------------------------------------------------
Pb(CO3)2--                Pb(CO3)2--
     charge  =  -2.0
****
     3 element(s):
      1.0000 Pb             2.0000 C             6.0000 O
****
     4 species in aqueous dissociation reaction:
    -1.0000  Pb(CO3)2--               -2.0000  H+
     1.0000  Pb++                      2.0000  HCO3-

**** logK grid [0-25-60-100C @1.0132bar; 150-200-250-300C @Psat-H2O]:
        No_Data   10.5300   No_Data   No_Data
        No_Data   No_Data   No_Data   No_Data
* Source: Jang(2022)
+----------------------------------------------------------------
Pb(CO3)OH-                Pb(CO3)OH-
```


Information Only

```
     charge  =  -1.0
****
     4 element(s):
      1.0000 Pb              1.0000 C              4.0000 O
      1.0000 H
****
     5 species in aqueous dissociation reaction:
    -1.0000  Pb(CO3)OH-               -2.0000  H+
     1.0000  Pb++                      1.0000  HCO3-
     1.0000  H2O
*
**** logK grid [0-25-60-100C @1.0132bar; 150-200-250-300C @Psat-H2O]:
        No_Data   13.4200   No_Data   No_Data
        No_Data   No_Data   No_Data   No_Data
* Source: Jang(2022)
+---------------------------------------------------------------
Pb(CO3)3----              Pb(CO3)3----
     charge  =  -4.0
****
     3 element(s):
      1.0000 Pb              3.0000 C              9.0000 O
****
     4 species in aqueous dissociation reaction:
    -1.0000  Pb(CO3)3----             -3.0000  H+
     1.0000  Pb++                      3.0000  HCO3-

**** logK grid [0-25-60-100C @1.0132bar; 150-200-250-300C @Psat-H2O]:
        No_Data   27.1900   No_Data   No_Data
        No_Data   No_Data   No_Data   No_Data
* Source: Jang(2022)
+---------------------------------------------------------------
+---------------------------------------------------------------
solids
+---------------------------------------------------------------
Am(OH)3(am)               Am(OH)3(am)
     V0PrTr  =   000.000 cm**3/mol [source:         ]
****
     3 element(s):
      1.0000 Am              3.0000 O              3.0000 H
****
     4 species in aqueous dissociation reaction:
    -1.0000  Am(OH)3(am)              -3.0000  H+
     1.0000  Am+++                     3.0000  H2O

**** logK grid [0-25-60-100C @1.0132bar; 150-200-250-300C @Psat-H2O]:
        No_Data   16.9000   No_Data   No_Data
        No_Data   No_Data   No_Data   No_Data
* Source: Guillaumont et al (2003)
+---------------------------------------------------------------
Fe(OH)2(s)                Fe(OH)2
     V0PrTr  =   000.000 cm**3/mol [source:         ]
****
     3 element(s):
      1.0000 Fe              2.0000 O              2.0000 H
****
     4 species in aqueous dissociation reaction:
    -1.0000  Fe(OH)2(s)               -2.0000  H+
     1.0000  Fe++                      2.0000  H2O

**** logK grid [0-25-60-100C @1.0132bar; 150-200-250-300C @Psat-H2O]:
        No_Data   12.8900   No_Data   No_Data
        No_Data   No_Data   No_Data   No_Data
* Source: Kim et al (2017)
```


Information Only

```
+------------------------------------------------------------------
Hibbingite                Fe2Cl(OH)3
     V0PrTr  =   000.000 cm**3/mol [source:         ]
****
     4 element(s):
      2.0000 Fe             1.0000 Cl             3.0000 H
      3.0000 O
****
     5 species in aqueous dissociation reaction:
    -1.0000  Hibbingite               -3.0000  H+
     2.0000  Fe++                      1.0000  Cl-
     3.0000  H2O
*
**** logK grid [0-25-60-100C @1.0132bar; 150-200-250-300C @Psat-H2O]:
        No_Data   17.0800   No_Data   No_Data
        No_Data   No_Data   No_Data   No_Data
* Source: Kim et al (2017)
+------------------------------------------------------------------
Siderite                  FeCO3
     V0PrTr  =   000.000 cm**3/mol [source:         ]
****
     3 element(s):
      1.0000 Fe             3.0000 O             1.0000 C
****
     4 species in aqueous dissociation reaction:
    -1.0000  Siderite                 -1.0000  H+
     1.0000  Fe++                      1.0000  HCO3-
*
**** logK grid [0-25-60-100C @1.0132bar; 150-200-250-300C @Psat-H2O]:
        No_Data  -0.1200   No_Data   No_Data
        No_Data   No_Data   No_Data   No_Data
* Source: Kim et al (2017), Stumm and Morgan (1996)
+------------------------------------------------------------------
Chukanovite               Fe2(OH)2CO3
     V0PrTr  =   000.000 cm**3/mol [source:         ]
****
     4 element(s):
      2.0000 Fe             5.0000 O             2.0000 H
      1.0000 C
****
     5 species in aqueous dissociation reaction:
    -1.0000  Chukanovite              -3.0000  H+
     2.0000  Fe++                      1.0000  HCO3-
     2.0000  H2O

**** logK grid [0-25-60-100C @1.0132bar; 150-200-250-300C @Psat-H2O]:
        No_Data   12.3200   No_Data   No_Data
        No_Data   No_Data   No_Data   No_Data
* Source: Kim et al (2017)
+------------------------------------------------------------------
Szomolnokite              FeSO4.H2O
     V0PrTr  =   000.000 cm**3/mol [source:         ]
****
     4 element(s):
      1.0000 Fe             1.0000 S             5.0000 O
      2.0000 H
****
     4 species in aqueous dissociation reaction:
    -1.0000  Szomolnokite             1.0000  Fe++
     1.0000  SO4--                    1.0000  H2O
*
**** logK grid [0-25-60-100C @1.0132bar; 150-200-250-300C @Psat-H2O]:
        No_Data  -0.9000   No_Data   No_Data
```


Information Only

```
        No_Data   No_Data   No_Data   No_Data
* Source: Reardon and Beckie (1987)
+---------------------------------------------------------------
Melanterite                FeSO4.7H2O
     V0PrTr  =   000.000 cm**3/mol [source:         ]
****
     4 element(s):
      1.0000 Fe             1.0000 S             11.0000 O
     14.0000 H
****
     4 species in aqueous dissociation reaction:
    -1.0000  Melanterite               1.0000  Fe++
     1.0000  SO4--                     7.0000  H2O

**** logK grid [0-25-60-100C @1.0132bar; 150-200-250-300C @Psat-H2O]:
        No_Data  -2.2000    No_Data   No_Data
        No_Data   No_Data   No_Data   No_Data
* Source: Reardon and Beckie (1987)
+---------------------------------------------------------------
Cotunnite                  PbCl2
     V0PrTr  =   000.000 cm**3/mol [source:         ]
****
     2 element(s):
      2.0000 Cl             1.0000 Pb
****
     3 species in aqueous dissociation reaction:
    -1.0000  Cotunnite                 1.0000  Pb++
     2.0000  Cl-
*
**** logK grid [0-25-60-100C @1.0132bar; 150-200-250-300C @Psat-H2O]:
        No_Data  -4.8300    No_Data   No_Data
        No_Data   No_Data   No_Data   No_Data
* Source: Jang et al (2021) in agreement with Edwards et al. (1992)
+---------------------------------------------------------------
Cerussite                  PbCO3
     V0PrTr  =   000.000 cm**3/mol [source:         ]
****
     3 element(s):
      1.0000 Pb             1.0000 C             3.0000 O
****
     4 species in aqueous dissociation reaction:
    -1.0000  Cerussite                -1.0000  H+
     1.0000  Pb++                      1.0000 HCO3-

**** logK grid [0-25-60-100C @1.0132bar; 150-200-250-300C @Psat-H2O]:
        No_Data  -2.8500    No_Data   No_Data
        No_Data   No_Data   No_Data   No_Data
* Source: Jang(2022)
+---------------------------------------------------------------
Abellaite                  NaPb2(CO3)2(OH)
     V0PrTr  =   000.000 cm**3/mol [source:         ]
****
     5 element(s):
      1.0000 Na             2.0000 Pb            2.0000 C
      7.0000 O              1.0000 H
****
     6 species in aqueous dissociation reaction:
    -1.0000  Abellaite                -3.0000  H+
     2.0000  Pb++                      2.0000  HCO3-
     1.0000  H2O                       1.0000  Na+

**** logK grid [0-25-60-100C @1.0132bar; 150-200-250-300C @Psat-H2O]:
        No_Data   2.5900    No_Data   No_Data
```


Information Only

```
        No_Data   No_Data   No_Data   No_Data
* Source: Jang (2022)
+---------------------------------------------------------------------
Hydrocerussite             2PbCO3.Pb(OH)2
     V0PrTr  =   000.000 cm**3/mol [source:         ]
****
     4 element(s):
      3.0000 Pb             2.0000 C              8.0000 O
      2.0000 H
****
     5 species in aqueous dissociation reaction:
    -1.0000  Hydrocerussite           -4.0000  H+
     3.0000  Pb++                      2.0000  HCO3-
     2.0000  H2O

**** logK grid [0-25-60-100C @1.0132bar; 150-200-250-300C @Psat-H2O]:
        No_Data   2.4100    No_Data   No_Data
        No_Data   No_Data   No_Data   No_Data
* Source: Jang (2022)
+---------------------------------------------------------------------
Anglesite                  PbSO4(s)
     V0PrTr  =   000.000 cm**3/mol [source:         ]
****
     3 element(s):
      1.0000 Pb             1.0000 S              4.0000 O
****
     3 species in aqueous dissociation reaction:
    -1.0000  Anglesite                1.0000  Pb++
     1.0000  SO4--

**** logK grid [0-25-60-100C @1.0132bar; 150-200-250-300C @Psat-H2O]:
        No_Data  -7.7700    No_Data   No_Data
        No_Data   No_Data   No_Data   No_Data
* Source: Jang (2023)
+---------------------------------------------------------------------
Hydromagnesite5424        Mg5(CO3)4(OH)2.4H2O
     V0PrTr  =   000.000 cm**3/mol [source:         ]
****
     4 element(s):
      4.0000 C             10.0000 H              5.0000 Mg
     18.0000 O
****
     5 species in aqueous dissociation reaction:
    -1.0000  Hydromagnesite5424       -6.0000  H+
     5.0000  Mg++                      4.0000  HCO3-
     6.0000  H2O
*
**** logK grid [0-25-60-100C @1.0132bar; 150-200-250-300C @Psat-H2O]:
        No_Data   31.4900   No_Data   No_Data
        No_Data   No_Data   No_Data   No_Data
* Source: Robie & Hemmingway (1973)
+---------------------------------------------------------------------
Earlandite                 Ca3Citrate2.4H2O
     V0PrTr  =   000.000 cm**3/mol [source:         ]
****
     4 element(s):
      3.0000 Ca            12.0000 C              18.0000 H
     18.0000 O
****
     4 species in aqueous dissociation reaction:
    -1.0000  Earlandite               3.0000  Ca++
     2.0000  Citrate---               4.0000  H2O
```


Information Only

```
**** logK grid [0-25-60-100C @1.0132bar; 150-200-250-300C @Psat-H2O]:
        No_Data  -17.9000   No_Data   No_Data
        No_Data   No_Data   No_Data   No_Data
* Source: Hummel et al (2005)
+---------------------------------------------------------------------
Glushinskite              MgOxalate.2H2O
     V0PrTr  =   000.000 cm**3/mol [source:         ]
****
     4 element(s):
      1.0000 Mg             2.0000 C              6.0000 O
      4.0000 H
****
     4 species in aqueous dissociation reaction:
    -1.0000  Glushinskite              1.0000  Mg++
     1.0000  Oxalate--                 2.0000  H2O

**** logK grid [0-25-60-100C @1.0132bar; 150-200-250-300C @Psat-H2O]:
        No_Data  -6.4900    No_Data   No_Data
        No_Data   No_Data   No_Data   No_Data
* Source: Jang et al (2021)
+---------------------------------------------------------------------
references
+---------------------------------------------------------------------
```


A
Altmaier, M., Metz, V., Neck, V., Muller, R., and Fanghanel, T., 2003. Solid-liquid equilibria of Mg(OH)2(cr) and Mg2(OH)3Cl.4H2O(cr) in the system Mg-Na-H-OH-O-Cl-H2O at 25 oC. Geochimica et Cosmochimica Acta 67, 3595-3601.

B
Borkowski, M., Moore, R. C., Bronikowski, M. G., Chen, J., Pokrovsky, O. S., Xia, Y., and Choppin, G. R., 2001. Thermodynamic modeling of actinide complexation with oxalate at high ionic strength. Journal of Radioanalytical and Nuclear Chemistry 248, 467-471.

C
Choppin, G. R., Bond, A. H., Borkowski, M., Bronikowski, M. G., Chen, J. F., Lis, S., Mizera, J., Pokrovsky, O., Wall, N. A., Xia, Y.-X., and Moore, R. C., 2001. Waste Isolation Pilot Plant Actinide Source Term Test Program: Solubility Studies and Development of Modeling Parameters. Sandia Report, SAND99-0943. Sandia National Laboratories.
Clegg, S. L., and P. Brimblecombe, 1990. The solubility and activity coefficient of oxygen in salt solutions and brines. Geochimica et Cosmochimica Acta, 54(12), 3315-3328.

D
None

E
None

F
Fanghanel, Th., J. I. Kim, P. Paviet, R. Klenze, and W. Hauser, 1994. Thermodynamics of radioactive trace elements in concentrated electrolyte solutions: hydrolysis of Cm3+ in NaCl-solutions. Radiochimica Acta, 66/67, 81-87.
Fanghanel, T., Neck, V., and Kim, J. I., 1995. Thermodynamics of Neptunium(V) In Concentrated Salt-Solutions .2. Ion-Interaction (Pitzer) Parameters for Np(V) Hydrolysis Species and Carbonate Complexes. Radiochimica Acta 69, 169-176.
Fanghanel, Th., and Kim, J. I., 1998. Spectroscopic evaluation of thermodynamics of trivalent actinides in brines. Journal of Alloys and Compounds, v.271--73, 728-737.
Fanghanel, Th., Th. Konnecke, H. Weger, P. Paviet-Hartmann, V. Neck, and J. I. Kim, 1999. Thermodynamics of Cm(III) in concentrated salt solutions: Carbonate complexation in NaCl solution at 25 °C, Journal of Solution Chemistry, v.28, no.4, 447-462.

Information Only

Felmy, A. R. and Weare, J. H., 1986. The prediction of borate mineral equilibria in natural waters: Application to Searles Lake, California. Geochimica et Cosmochimica Acta 50, 2771--783.
Felmy, A. R., D. Rai, and R. W. Fulton. 1990. The solubility of AmOHCO3(c) and the aqueous thermodynamics of the system Na+ - Am3+ - HCO3- - CO32- - OH- - H2O. Radiochimica Acta, 50, 193--04.
Felmy, A. R., D. Rai, and M. J. Mason. 1991. The Solubility of Hydrous Thorium(IV) Oxide in Chloride Media: Development of an Aqueous Ion-Interaction Model. Radiochimica Acta, 55, 177-185.
Felmy, A. R., and D. Rai, 1992. An Aqueous Thermodynamic Model for a High Valence 4:2 Electrolyte Th4+ - SO42- in the System Na+ - K+ - Li+ - NH4+ - Th4+ - SO42- - HSO4- - H2O to High Concentration. Journal of Solution Chemistry, 21(5), 407-423.
Felmy, A. R., D. Rai, S. M. Sterner, M. J. Mason, N. J. Hess, and S. D. Conradson, 1997. Thermodynamic Models for Highly Charged Aqueous Species: Solubility of Th(IV) Hydrous Oxide in Concentrated NaHCO3 and Na2CO3 Solutions. Journal of Solution Chemistry, 26(3), 233--48.
Felmy, A. R., and D. Rai, 1999. Application of Pitzer's Equations for Modeling the Aqueous Thermodynamics of Actinide Species in Natural Waters: A Review. Journal of Solution Chemistry, 28(5), 533-553.

G
Giambalvo, E. R., 2002, Org. Recommended Parameter Values for Modeling Organic Ligands in WIPP Brines. Memo to Laurence H. (Larry) Brush., July 25, 2002. ERMS 522981.
Giambalvo, E. R., 2002, Oxalate. Recommended u0/RT values for modeling the solubility of oxalate solids in WIPP brines. Memo to Laurence H. Brush, July 31, 2002. Sandia National Laboratories, Carlsbad, New Mexico, U.S.A. ERMS 523057.
Giambalvo, E. R., 2002, An(III). Recommended Parameter Values for Modeling An(III) Solubility in WIPP Brines. Memo to Laurence H. Brush, July 25, 2002. ERMS 522982.
Giambalvo, E. R., 2002, An(IV). Recommended Parameter Values for Modeling An(IV) Solubility in WIPP Brines. Memo to Laurence H. Brush, July 26, 2002. ERMS 522986.
Giambalvo, E. R., 2002, An(V). Recommended Parameter Values for Modeling An(V) Solubility in WIPP Brines. Memo to Laurence H. (Larry) Brush, July 26, 2002. ERMS 522990.
Giambalvo, E. R., 2003, FMT. Release of FMT database FMT_021120.CHEMDAT. Memo to Laurence H. (Larry) Brush, March 10, 2003. Sandia National Laboratories, Carlsbad, New Mexico, U.S.A. ERMS 526372.

H
Harvie, C. E., Møller, N., and Weare, J. H., 1984. The prediction of mineral solubilities in natural waters: The Na-K-Mg-Ca-H-Cl-SO4-OH-HCO3-CO3-CO2-H2O system to high ionic strengths at 25°C. Geochimica et Cosmochimica Acta 48, 723-751.

I
None

J
Jang, J., 2021. Revisit to the Pitzer Geochemical Thermodynamic Model for the PbCl2(s)-HCl-H2O System. Sandia National Laboratories, Carlsbad, NM, USA. ERMS 575309.

Jang, J., P. Hora, L. Kirkes, C. Miller, and L. Zhang, 2021. Analysis Report documenting Solubility and Complexation of Iron, Lead, Magnesium, Neodymium, and Boron in the WIPP-Relevant Brines under TPs 06-03, 08-02, 12-02, 14-03, 14-05, 16-02, 19-01, and 20-01. Revision 0. GEOC-21-11. Sandia National Laboratories, Carlsbad, New Mexico, U.S.A. ERMS 576381. SAND2022-13723R.

Jang, J., 2022. The PbCO3(s) - NaHCO3 - Na2CO3 - H2O Experiment (Revision 0): Addendum to Xiong (2015a,b). Memo to SNL WIPP Records Center and SNL WIPP Geochemistry. December 2, 2022. Sandia National Laboratories, Carlsbad, New Mexico, U.S.A. ERMS 578642.

Information Only

Jang, J., 2023. The PbSO4(s) - Na2SO4 - NaCl - H2O Experiment (Revision 0). Memo to SNL WIPP Records Center, SNL WIPP Geochemistry.
January 30, 2023. Sandia National Laboratories, Carlsbad, New Mexico, U.S.A. ERMS 578721.

Jang, J., and I. Foli, 2023. Solubility and Complexation of Iron, Lead, Magnesium, Neodymium, Boron, and Calcium in Brines, Revision 1
of GEOC-21-11. GEOC-22-01/03/09. Sandia National Laboratories, Carlsbad, New Mexico. February 1, 2023. ERMS PENDING.

K
Konnecke, Th., Th. Fanghanel, and J. I. Kim, 1997. Thermodynamics of trivalent actinides in concentrated electrolyte solutions: Modelling the chloride complexation of Cm(III), Radiochimica Acta, 76, 131-135.

L
None

M
Moore, R. C., M. Borkowski, M. G. Bronikowski, J. Chen, O. S. Pokrovsky, Y. Xia, and G. R. Choppin, 1999. Thermodynamic modeling of actinide complexation with acetate and lactate at high ionic strength. Journal of Solution Chemistry, v.28, no.5, 521-531.

N
Neck, V., Fanghanel, T., Rudolph, G., and Kim, J. I., 1995. Thermodynamics of Neptunium(V) in Concentrated Salt Solutions: Chloride Complexation and Ion Interaction (Pitzer) Parameters for the NpO2+ Ion. Radiochimca Acta, 69, 39-47.
Neck, V., R. Muller, M. Bouby, M. Altmaier, J. Rothe, M. A. Denecke, and J. I. Kim, 2002. Solubility of amorphous Th(IV) hydroxide - application of LIBD to determine the solubility product and EXAFS for aqueous speciation. Radiochimica Acta, 90, 485-494.
Novak, C. F., 1995. Creation and Definition of the Database for FMT called "HMW_NP_AM.CHEMDAT," version date 94.01.17. Memo to Nancy J. Dhooge, 18 January 1995, Sandia National Laboratories, Albuquerque, New Mexico, U.S.A. WPO 20130.
Novak, C. F., 1996. Preliminary Inorganic Model for Thorium Solubility in WIPP Brines, in database file HMW_3TH5_960119.CHEMDAT. Memo to E. J. Nowak, 19 January 1996. Sandia National Laboratories, Albuquerque, New Mexico. WPO 30930.
Novak, C. F., Borkowski, M., and Choppin, G. R., 1996. Thermodynamic Modeling of Neptunium(V)-Acetate Complexation in Concentrated NaCl Media Radiochimca Acta. 74, 111-116.
Novak, C. F., I. Al Mahamid, K. A. Becraft, S. A. Carpenter, N. Hakem, and T. Prussin, 1997. Measurement and thermodynamic modeling of Np(V) solubility in aqueous K2CO3 solutions to high concentrations. Journal of Solution Chemistry, vol.26, no.7, 681-697.
Nowak, E. J., 2005. Recommended Change in the FMT Thermodynamic Data Base. Memo to Laurence H. (Larry) Brush, April 1, 2005. Sandia National Laboratories, Carlsbad, New Mexico, U.S.A. ERMS 539227.
O
None

P
Pitzer, K. S., 1991. Ion interaction approach: Theory and data correlation. In: Pitzer, K. S. (Ed.), Activity Coefficients in Electrolyte Solutions, 2nd Edition. CRC Press, Boca Raton, Florida.
Pitzer, K. S. and Silvester, L. F., 1976. Thermodynamics of electrolytes. VI. Weak electrolytes including H3PO4. Journal of Solution Chemistry, 5, 269--78.
Pokrovsky, O. S., Bronikowski, M. G., Moore, R. C., and Choppin, G. R., 1998. Interaction of Neptunyl(V) and Uranyl(VI) with EDTA in NaCl Media: Experimental Study and Pitzer Modeling. Radiochimca Acta 80, 23.

Q
None

R

Information Only

Rai, D., A. R. Felmy, and R. W. Fulton, 1992a. Solubility and Ion Activity Product of AmPO4.xH2O(am). Radiochimica Acta, 56, 7-14.
Rai, D., A. R. Felmy, R. W. Fulton, and J. L. Ryan, 1992b. Aqueous Chemistry of Nd in Borosilicate-Glass/Water Systems. Radiochimica Acta, 58/59, 9-16.
Rai, D., A. R. Felmy, and R. W. Fulton, 1995a. Nd3+ and Am3+ ion interactions with sulfate ion and their influence on NdPO4(c) solubility. Journal of Solution Chemistry, 24(9), 879-895.
Rai, D., A. R. Felmy, S. M. Sterner, D. A. Moore, M. J. Mason, and C. F. Novak, 1997. The Solubility of Th(IV) and U(IV) Hydrous Oxides in Concentrated NaCl and MgCl2 Solutions. Radiochimica Acta, 79, 239--47.
Robie, R. A., and B. S. Hemingway, 1973. The Enthalpies of Formation of Nesquehonite, MgCO3.3H2O and Hydromagnesite, 5MgO.4CO2.5H2O. Journal of Research of the U.S. Geological Survey, 1(5), 543-547.
Roy, R. N., Vogel, K. M., Good, C. E., Davis, W. B., Roy, L. N., Johnson, D. A., Felmy, A. R., and Pitzer, K. S., 1992. Activity coefficients in electrolyte mixtures: HCl + ThCl4 + H2O for 5-55 °C. The Journal of Physical Chemistry, 96, 11065-11072.

S
Shock, E. L., and H. C. Helgeson, 1988. Calculation of the Thermodynamic and Transport Properties of Aqueous Species at High Pressures and Temperatures: Correlation Algorithms for Ionic Species and Equation of State Predictions to 5 kb and 1000°C." Geochimica Cosmochimica Acta, 52(8), 2009--036.

T
None

U
None

V
None

W
Wolery, T. J. and C. Jove-colon. 2007. Qualification of Thermodynamic Data for Geochemical Modeling of Mineral-Water Interactions in Dilute Systems. ANL-WIS-GS-000003 REV 01. DTN: SN0612T0502404.014.

X
Xiong, Y., 2004. A correction of the molecular weight of oxalate in FMT_021120.CHEMDAT, and Incorporation of calcium oxalate monohydrate (Whewellite) into CHEMDAT with its recommended dimensionless standard chemical potential value. Memo to Larry Brush, June 8, 2004, Sandia National Laboratories, Carlsbad, New Mexico, U.S.A. ERMS 535813.
Xiong, Y., 2005. Release of FMT_050405.CHEMDAT. Email to J. F. Kanney, J. J. Long, Copied to M. J. Chavez, L. H. Brush, 'Jim Nowak', E. J. Nowak, April 05, 2005, with an attachment "compare.txt". ERMS 539304.
Xiong, Y., H. Deng, M. Nemer, and S. Johnsen, 2010. Experimental determination of the solubility constant for magnesium chloride hydroxide hydrate (Mg3Cl(OH)5·4H2O, phase 5) at room temperature, and its importance to nuclear waste isolation in geological repositories in salt formations. Geochimica et Cosmochimica Acta 74(16), 4605-4611.
Xiong, Y., 2011. Release of EQ3/6 Database DATA0.FM1. Email to Jennifer Long, March 9, 2011. Sandia National Laboratories, Carlsbad, New Mexico. ERMS 555152.

Y
None

Z
None

stop.
+---
Miscellaneous Notes

Information Only

```
endit.

+-------------------------------------------------------------------
```


Information Only

579803

Sandia National Laboratories

Operated for the United States Department of Energy
National Nuclear Security Administration
by National Technology and Engineering
Solutions of Sandia, LLC.
Albuquerque, New Mexico 87185-0143
Livermore, California 94551-0969

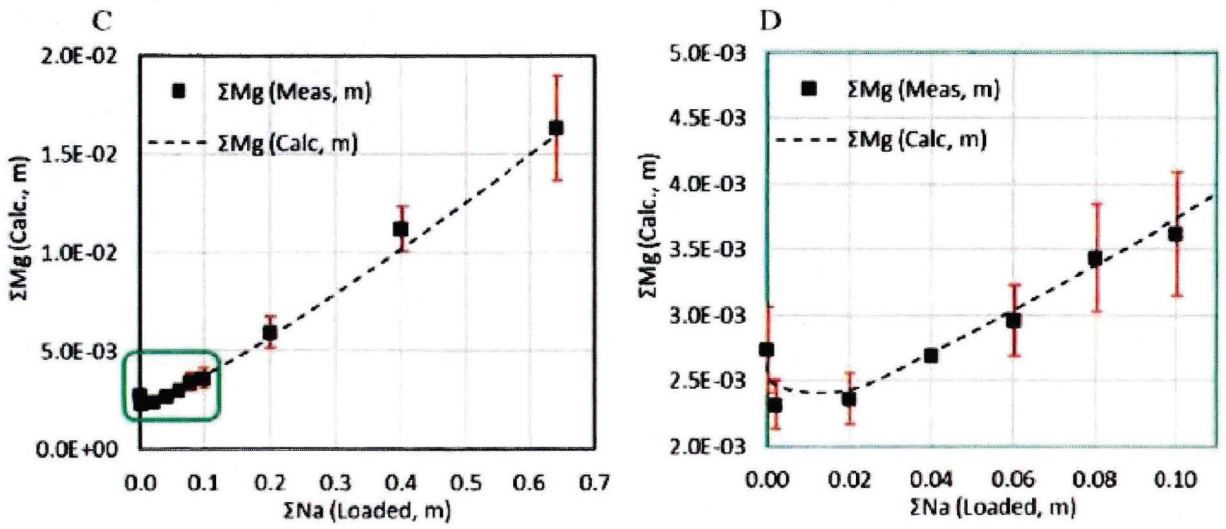
date: June 27, 2023

to: SNL WIPP Records Center
Defense Waste Management Programs

from: Paul Domski *signature on file*

subject: Memo of Correction: Corrections to Section 3.1.3 of the Analysis Report: *An Update to the WIPP EQ3/6 Database DATA0.FM1 with the Creation of DATA0.FM6*

In the period after the analysis report *"An Update to the WIPP EQ3/6 Database DATA0.FM1 with the Creation of DATA0.FM6"* was submitted into WIPP records three non-quality affecting errors were identified in the report. These errors did NOT affect the glushinskite parameters included in DATA0.FM6 (Domski, 2023a), and therefore, did not impact subsequent actinide solubility calculations or uncertainty analysis using DATA0.FM6. The issue was specific to the report only, and had to do with the mineral phase glushinskite [MgOxalate·2H_2O(s)], the first (1) was a typo in the caption for Figure 11, the second and third errors were the use of the dissociation reaction for the Mg – oxalate aqueous species ($Mg(Oxalate)_2^{2-}$) (2) in the text of the report, and (3) in the calculation of the apparent solubility product (log Ksp,app) for glushinskite. The third issue, calculation of log Ksp,app for glushinskite, affected the values in Table 14 and Figure 12 of the report. The updated text, table, and figure are presented below:



Information Only

Figure 11. Reproduction of Figure VI.1-10, parts C and D from Jang et al. (2021b). Parametrization of $MgOxalate{\cdot}2H_2O(s) - Na_2Oxalate - H_2O$ system. Fitting of the model using the new recommended glushkinskite log Ksp. D is a zoomed-in view of the green rectangle in C.

To build additional confidence in the glushinskite solubility product its apparent solubility product based on the experimental data (Table VI.1-10, Jang et al., 2021b) and the EQ3NR model response was calculated. The results are plotted in Figure 12, and the method used to calculate the apparent log K is presented below.

The dissolution reaction for glushinskite can be written as:

$MgOxalate{\cdot}2H_2O(s)$ (Glushinskite) $\rightleftharpoons Mg^{2+} + Oxalate^{2-} + 2H_2O$

The apparent solubility product is given by:

$Ksp,app = [Mg^{2+}] \times [Oxalate^{2-}]$

By definition, the activity of a pure solid is equal to 1. The activity of water is purposely set equal to 1 for simplicity of calculation of Ksp,app. Note the square brackets ([-]) indicate concentration in units of molality (m).

The $\log_{10}$ of the apparent solubility product is then given by

$\log Ksp,app = \log [Mg^{2+}] + \log[Oxalate^{2-}]$

Table 14 provides the pmH, Mg, Na, and oxalate molalities used to calculate the log Ksp,app values for glushinskite as a function of sodium concentration for the experimental and simulated values.

Table 1. Apparent Log K values for Glushinskite.

Measured Data from Jang et al. (2021b), Table VI.1-10					**EQ3NR Simulated Data**				
pmH	**Mg (m)**	**Na (m)**	**Oxalate (m)**	**logKsp,app**	**pmH**	**Mg (m)**	**Na (m)**	**Oxalate (m)**	**logKsp,app**
8.34	2.74E-03	5.36E-04	5.33E-03	-4.84	8.34	2.35E-03	5.36E-03	5.03E-03	-4.93
8.31	2.32E-03	4.07E-03	2.56E-03	-5.23	8.31	2.38E-03	4.07E-03	4.41E-03	-4.98
8.13	2.36E-03	1.98E-02	9.27E-03	-4.66	8.13	2.44E-03	1.98E-02	1.23E-02	-4.52
8.19	2.69E-03	6.65E-02	2.15E-02	-4.24	8.19	3.16E-03	6.65E-02	3.64E-02	-3.94
8.26	2.96E-03	8.29E-02	3.19E-02	-4.02	8.26	3.44E-03	8.29E-02	4.49E-02	-3.81
8.27	3.43E-03	1.00E-01	4.21E-02	-3.84	8.27	4.11E-03	1.19E-01	6.36E-02	-3.58
8.29	3.62E-03	1.19E-01	5.21E-02	-3.72	8.29	6.15E-03	2.20E-01	1.16E-01	-3.15
8.37	5.94E-03	2.20E-01	1.04E-01	-3.21	8.37	1.04E-02	4.09E-01	2.15E-01	-2.65
8.49	1.11E-02	4.09E-01	2.27E-01	-2.60	8.49	1.35E-02	5.37E-01	2.82E-01	-2.42
8.59	1.63E-02	5.37E-01	2.61E-01	-2.37	8.59	1.35E-02	5.38E-01	2.82E-01	-2.42

Information Only

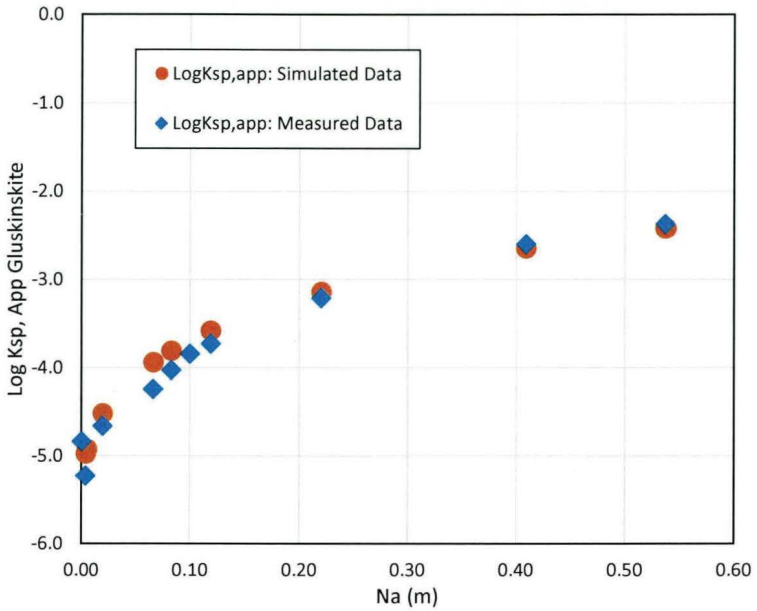


Figure 12. Apparent Log Ksp values for the glushinskite measured data compared to the model predicted apparent Log Ksp values.

The spreadsheet *"Python_LogKsp,app_FM6-Verification.xlsx"* was updated and will replace the version included in the records package. This file is stored at: /data/cvs/CVSLIB/WIPP_EXTERNAL/ap200/Files.

This memo of correction was issued to correct three errors identified in the analysis report *"An Update to the WIPP EQ3/6 Database DATA0.FM1 with the Creation of DATA0.FM6"*. None of the errors identified were quality affecting and had zero impact on the parameter values included in the WIPP thermodynamic database DATA0.FM6 (Domski, 2023a), and subsequently had no impact on the RPPCR baseline solubility calculations (Domski, 2023b), or actinide uncertainty analysis (Domski, 2023c).

References

Domski, P. S. 2023a. "An Update to the WIPP EQ3/6 Pitzer Thermodynamic Database DATA0.FM1 with the Creation of DATA0.FM6". Sandia National Laboratories, Carlsbad, New Mexico. ERMS 579370.

Domski, P.S. 2023b. "Prediction of Baseline Actinide Solubilities for the Replacement Panels Planned Change Request (RPPCR) Performance Assessment". Carlsbad, NM: Sandia National Laboratories. ERMS 579503.

Domski, P.S. 2023c. "Uncertainty Analysis of Actinide Solubilities for the Replacement Panels Planned Change Request (RPPCR) Performance Assessment and the 2024 Compliance Recertification Application (CRA-2024)". Carlsbad, NM: Sandia National Laboratories. ERMS 579525.

WIPP:4.4.2.2.1:TD:QA-L:RECERT:579369
Information Only